Article Pre-Print

INTERNATIONAL JOURNAL OF ROBUST AND NONLINEAR CONTROL

Int. J. Robust. Nonlinear Control 2010; **00**:1–36

Published online in Wiley InterScience (www.interscience.wiley.com). DOI: 10.1002/rnc

Actuator and sensor fault detection and isolation for nonlinear systems subject to uncertainty

Hadi Shahnazari, Prashant Mhaskar*

Department of Chemical Engineering, 1280 Main Street West, Hamilton, ON L8S 4L7 Canada

SUMMARY

This work considers the problem of actuator and sensor fault diagnosis for nonlinear uncertain systems. The key idea is to detect and isolate faults by using a bank of filters, with thresholds defined in a way that they explicitly account for the effect of uncertainty. To this end, first the ability of high gain observer in providing bounded estimation error for a generalized class of nonlinear uncertain systems is rigorously established. Utilizing these bounds, thresholds are defined in a way that they account for the impact of uncertainty on each residual. In this way, each residual remains insensitive to a subset of fault scenarios in the presence of uncertainty and sensitive to the rest, if the corresponding detectability conditions are satisfied. This enables fault detection and isolation (FDI) in the presence of uncertainty by resulting in a unique breaching pattern in residuals corresponding to each fault scenario. The fault detectability and isolability conditions for the proposed FDI scheme are rigorously derived. The efficacy of the fault detection and isolation framework subject to uncertainty and measurement noise is illustrated using a chemical reactor example. Copyright © 2010 John Wiley & Sons, Ltd.

Received . . .

KEY WORDS: Uncertainty; Fault diagnosis; Actuator faults; Sensor faults; Nonlinear systems; High-gain observers

*Correspondence to: Department of Chemical Engineering, 1280 Main Street West, Hamilton, ON L8S 4L7 Canada.
†

1. INTRODUCTION

Fault detection and isolation are critical components of a fault tolerant control system, and are becoming more and more important given the ubiquitousness of automation- from process industries to self-driven vehicles. Given the system complexity and disturbances, the FDI design must account for effect of system nonlinearity and uncertainty, motivating a number of results in this direction.

The FDI problem explicitly accounting for nonlinear systems has been considered widely in the literature during the past decade (see, e.g., [1], [2], [3], [4], [5], [6], [7], [8] and [9]). In [7], sensor fault isolation, and in [6] distinguishing between sensor and actuator, both in the absence of uncertainty, is addressed.

For nonlinear uncertain systems, in [10], the problem of isolation of actuator (only, not sensor) faults in the presence of uncertainty is handled by explicitly characterizing the way the faults affect the nonlinear process system, and driving the system to a point that enables fault isolation. In [11], a geometric approach is employed for a class of nonlinear systems to decouple effect of uncertainty and fault (only actuator faults are considered) using sliding mode observers. In [12], under certain matching conditions, sliding mode observers are designed to reconstruct actuator fault signals. The problem of FDI in the presence of uncertainty has also been studied using adaptive estimation techniques (see e.g., [13], [14] and [15]). In these approaches, first a fault detection scheme is designed which uses output estimation error as residual forming the basis of fault detection filters. The existing results, however, consider only single faults. In summary, there is a lack of results for nonlinear systems subject to uncertainty where the problem of fault detection and isolation for simultaneous actuator and sensor faults is addressed.

Motivated by the above considerations, this work considers the problem of actuator and sensor fault detection and isolation for nonlinear systems in the presence of uncertainty. This is achieved by building a bank of residuals, each using an appropriate subset of the available measurements (and associated state observers), to determine the expected behavior of the system and compare with the observed evolution, where each residual is sensitive to a subset of faults and insensitive to the rest, in the absence of uncertainty. To achieve FDI in the presence of uncertainty, thresholds are defined in

Prepared using rncauth.cls
DOI: 10.1002/rnc

a way that they account for the impact of the uncertainty on the estimation error and the prediction of the expected system behavior. In this way, each residual is still insensitive to a subset of faults in the presence of uncertainty and sensitive to the rest if the fault functionality satisfies a detectability condition. The rest of this manuscript is organized as follows: the system description is presented in Section 2. In Section 3, the boundedness of estimation error in the presence of uncertainty using high gain observers is rigorously established. In Section 4, the FDI mechanism is presented. In particular, thresholds are defined in a way they utilize the bound determined in Section 3 to ensure that there is no false alarms and the residuals retain their insensitive property in the presence of uncertainty. Then the detectability and isolability conditions for single and simultaneous faults are presented, when the detectability analysis establishes that the sensitive property of residuals is retained in the presence of uncertainty. The efficacy of proposed FDI framework in the presence of uncertainty and measurement noise is illustrated using a chemical reactor example in Section 5. Finally, Section 6 presents some concluding remarks.

2. PRELIMINARIES

Consider a multi-input multi-output nonlinear system described by

$$\begin{aligned} \dot{x} &= f(x) + G(x)(u + u_f) + \theta(x, u, t) \\ y &= h(x) + y_f \end{aligned} \tag{1}$$

where $x \in \mathcal{X} \subset \mathbb{R}^n$ denotes the vector of state variables, with $\mathcal{X}$ being a compact set of the admissible state values, $u = [u_1, \ldots, u_m]^{\mathrm{T}} \in \mathbb{R}^m$ denotes the vector of prescribed control inputs, taking values in a nonempty compact convex set $\mathcal{U} \subseteq \mathbb{R}^m$, $u_f = [u_{f_1}, \ldots, u_{f_m}]^{\mathrm{T}} \in \mathbb{R}^m$ denotes the unknown fault vector for the actuators, θ denotes the unstructured uncertainty with $\|\theta(x, u, t)\| \leq \bar{\theta}$, where $\bar{\theta}$ is a known positive constant, $y = [y_1, \ldots, y_p]^{\mathrm{T}} \in \mathbb{R}^p$ denotes the vector of output variables, $y_f = [y_{f_1}, \ldots, y_{f_p}]^{\mathrm{T}} \in \mathbb{R}^p$ denotes the unknown fault vector for the sensors and $G(x) = [g_1(x), \ldots, g_m(x)]$. The inputs are implemented in a discrete fashion, with sampling time Δ. Due to the presence of physical constraints, the actual input $u + u_f$ implemented to the system takes values from the set $\mathcal{U}$ as well and t_f denotes the time of fault occurrence. Throughout the manuscript,

Prepared using rncauth.cls
DOI: 10.1002/rnc

$L_f h(x)$ denotes the standard Lie derivative of a scalar function $h(x)$ with respect to a vector function $f(x)$ defined as $L_f h(x) = \frac{\partial f}{\partial x} \cdot h(x)$, and $\|\cdot\|$ denotes the Euclidean norm for the vectors.

Remark 1. Note that the above system description includes all kinds of uncertainty including parametric $\theta(t)$, structural uncertainty $\theta(x)$ and unstructured uncertainty $\theta(x, u, t)$. In particular, the system description allows those kinds of uncertainty which results from, for instance, the model having fewer number of states than the true system. Utilizing the bounds on the resultant uncertainty could admittedly be conservative, however, there simply exists no other method for rigorously handling these kinds of uncertainties. On the other hand, if the uncertainty is known to be parametric, the resulting tighter bounds on the uncertainty can readily be utilized.

3. BOUNDEDNESS OF ESTIMATION ERROR UNDER HIGH GAIN OBSERVERS IN THE PRESENCE OF UNCERTAINTY

The proposed fault detection and isolation mechanism involves observers, and in turn requires boundedness of state estimation error. In this section we utilize a high gain observer, and first establish boundedness of the estimation error in the presence of uncertainty. To this end, we consider the system of Eq. 1 under fault free conditions, satisfying Assumptions 1-3:

Assumption 1

The functions $f : \mathbb{R}^n \to \mathbb{R}^n$, $g_i : \mathbb{R}^n \to \mathbb{R}^n$, $i = 1, \ldots, m$, $\theta(x, u, t) : \mathbb{R}^n \to \mathbb{R}^n$ and $h : \mathbb{R}^n \to \mathbb{R}^p$ are smooth on their domains of definition, and $f(0) = 0$.

Assumption 2

For the system of Eq. (1), there exists a positive definite $\mathcal{C}^2$ function $V : \mathbb{R}^n \to \mathbb{R}$ such that for any $x \in \Omega_c := \{x \in \mathbb{R}^n : V(x) \leq c\}$, where c is a positive real number, the following inequality holds:

$$L_f V(x) + L_g V(x) u_c(x) + L_\theta V(x) \leq -\alpha(V(x)) \tag{2}$$

where $L_g V(x) = [L_{g_1} V(x), \ldots, L_{g_m} V(x)]$, $u_c : \Omega_c \to \mathcal{U}$ is a state feedback control law and α is a class $\mathcal{K}$ function.

Prepared using rncauth.cls
DOI: 10.1002/rnc

Remark 2. It is recognized that there exists no general procedure for construction of robust control Lyapunov functions (RCLFs) for nonlinear uncertain systems of Eq. 1. However, for several class of nonlinear uncertain system, such a procedure exists (see e.g., [16] for further details). This includes feedback linearizable systems and nonlinear systems in strict feedback form. More importantly, Assumption 2 simply states that a control design is in place to handle the uncertainly in the system, and does not require the knowledge of the specific Lyapunov function for the FDI design.

Assumption 3

There exist integers ω_i, $i = 1, \ldots, p$, with $\sum_{i=1}^{p} \omega_i = n$, and a coordinate transformation $\zeta = T(x,u,t) = T'(x,u) + T_\theta(x,u,t)$ such that if $u = \bar{u}$, where $\bar{u} \in \mathcal{U}$ is a constant vector, then the representation of the system of Eq. 1 in the ζ coordinate takes the following form:

$$\begin{aligned} \dot{\zeta} &= A\zeta + B\phi(\zeta, \bar{u}) + \eta(\zeta, \bar{u}, t) \\ y &= C\zeta \end{aligned} \tag{3}$$

where $\zeta = [\zeta_1, \ldots, \zeta_p]^{\mathrm{T}} \in \mathbb{R}^n$, $A = \text{blockdiag}[A_1, \ldots, A_p]$, $B = \text{blockdiag}[B_1, \ldots, B_p]$, $C = \text{blockdiag}[C_1, \ldots, C_p]$, $T' = \phi = [\phi_1, \ldots, \phi_p]^{\mathrm{T}}$, $T_\theta = \eta = [\eta_1, \ldots, \eta_p]^{\mathrm{T}}$, $\zeta_i = [\zeta_{i,1}, \ldots, \zeta_{i,\omega_i}]^{\mathrm{T}}$, $A_i = \begin{bmatrix} 0 & I_{\omega_i - 1} \\ 0 & 0 \end{bmatrix}$, with $I_{\omega_i - 1}$ being a $(\omega_i - 1) \times (\omega_i - 1)$ identity matrix, $B_i = [0^{\mathrm{T}}_{\omega_i - 1}, 1]^{\mathrm{T}}$, with $0_{\omega_i - 1}$ being a vector of zeros of dimension $\omega_i - 1$, $C_i = [1, 0^{\mathrm{T}}_{\omega_i - 1}]$, $\phi_i(\zeta, \bar{u}) = \phi_{i,\omega_i}(\zeta, \bar{u})$, with $\phi_{i,\omega_i}(\zeta, \bar{u})$ defined through the successive differentiation of $h_i(x)$: $\phi_{i,1}(\zeta, \bar{u}) = h_i(x)$ and $\phi_{i,j}(\zeta, \bar{u}) = \frac{\partial \phi_{i,j-1}}{\partial x}[f(x) + g(x)\bar{u}]$ and $\eta_i(\zeta, \bar{u}, t) = \eta_{i,\omega_i}(\zeta, \bar{u}, t)$, with $\eta_{i,\omega_i}(\zeta, \bar{u}, t)$ defined: $\eta_{i,1}(\zeta, \bar{u}, t) = 0$ and $\eta_{i,j}(\zeta, \bar{u}, t) = \frac{\partial \phi_{i,j-1}}{\partial x}[\theta(x,u,t)]$. Furthermore, $T' : \mathbb{R}^n \times \mathcal{U} \to \mathbb{R}^n$, $T_\theta : \mathbb{R}^n \times \mathcal{U} \to \mathbb{R}^n$, $T'^{-1} : \mathbb{R}^n \times \mathcal{U} \to \mathbb{R}^n$, and $T_\theta^{-1} : \mathbb{R}^n \times \mathcal{U} \to \mathbb{R}^n$ are $\mathcal{C}^1$ functions on their domains of definition, η denotes the uncertainty in the new coordinate system and $\|\eta(\zeta, u, t)\| \leq \bar{\eta}$, where $\bar{\eta}$ is a known positive constant.

We next describe the utilized high-gain observer formulation, which is coupled with sample-and-hold control. In the closed-loop system, the input is prescribed at discrete times $t_k = k\Delta$, $k = 0, \ldots, \infty$, with Δ being the hold-time of the control action. For $t \in [t_k, t_{k+1})$, the observer

Prepared using rncauth.cls
DOI: 10.1002/rnc

is formulated as follows ([7]):

$$\begin{aligned}\dot{\hat{\zeta}} &= A\hat{\zeta} + B\phi_0(\hat{\zeta}, u(t_k)) + H(y - C\hat{\zeta}) \\ \hat{\zeta}(t_k) &= T'(\hat{x}(t_k), u(t_k))\end{aligned} \tag{4}$$

where $\hat{x}$ and $\hat{\zeta}$ denote the estimates of x and ζ, respectively, $H = \text{blockdiag}[H_1, \ldots, H_p]$ is the observer gain, $H_i = \left[\frac{a_{i,1}}{\varepsilon}, \ldots, \frac{a_{i,\omega_i}}{\varepsilon^{\omega_i}}\right]^{\mathrm{T}}$, with $s^{\omega_i} + a_{i,1}s^{\omega_i - 1} + \cdots + a_{i,\omega_i} = 0$ being a Hurwitz polynomial and ε being a positive constant to be specified, $\hat{x}(t_k) = T'^{-1}(\hat{\zeta}(t_k^-), u(t_{k-1})))$ for $k = 1, \ldots, \infty$, and ϕ_0 is the nominal model of ϕ. The initial state of the observer is denoted by $\hat{x}_0 := \hat{x}(0)$, which takes values from any compact set $\mathcal{Q} \subseteq \mathbb{R}^n$. In the transformed coordinate, the state estimate $\hat{\zeta}$ is re-initialized at the discrete times to account for the possible discrete changes in the input and ensuring that the resulting state estimates remain continuous.

Remark 3. Assumption 3 provides a modified version of input-output normal form in the presence of uncertainty with unmeasured states being the inputs, measured states being the outputs with time derivative of measured states depending on transformed form of uncertainty in ζ coordinate and without requiring the dynamics to be affine in the unmeasured states. This, along with existing techniques to handle measurement noise (see e.g., [7] and [17]) significantly enhances the applicability of the designed observer. Benefiting from these, the assumptions on the dynamic system of Eq. 1 allow inclusion of a more general class of nonlinear systems compared to the previous designs (see e.g., [12] and [14]). In particular, no specific form for $f(x)$ and $g(x)$ (as in [14]), nor any additional assumptions on $\theta(x, u, t)$ (as in [12]) are imposed.

Another requirement is the global boundedness of ϕ_0 formalized in Assumption 4 below (with a choice of zero readily satisfying the assumption).

Assumption 4

[18] $\phi_0(\zeta, u)$ is a $\mathcal{C}^0$ function on its domain of definition and globally bounded in ζ.

Preparatory to the presentation of results on the convergence of the observer, we first state an important property of the scaled estimation error. To this end, let $D = \text{blockdiag}[D_1, \ldots, D_p]$, where $D_i = \text{diag}[\varepsilon^{\omega_i - 1}, \ldots, 1]$, and define the scaled estimation error $e = D^{-1}(\zeta - \hat{\zeta}) \in \mathbb{R}^n$. For

Prepared using rncauth.cls
DOI: 10.1002/rnc

$t \in [t_k, t_{k+1})$, the scaled estimation error evolves as follows:

$$\begin{aligned} \varepsilon \dot{e} &= A_0 e + \varepsilon B[\phi(\zeta, u(t_k)) - \phi_0(\hat{\zeta}, u(t_k))] + \varepsilon \eta(\zeta, u(t_k), t) \\ e(t_k) &= D^{-1}[T(x(t_k), u(t_k), t) - T'(\hat{x}(t_k), u(t_k), t)] \end{aligned} \tag{5}$$

where $A_0 = \text{blockdiag}[A_{0,1}, \ldots, A_{0,p}]$, $A_{0,i} = [a_i, b_i]$, $a_i = [-a_{i,1}, \ldots, -a_{i,\omega_i}]^{\mathrm{T}}$, and $b_i = [I_{\omega_i - 1}, 0_{\omega_i - 1}]^{\mathrm{T}}$.

Applying the change of time variable $\tau = \frac{t}{\varepsilon}$ and setting $\varepsilon = 0$, the boundary-layer system is given by

$$\frac{de}{d\tau} = A_0 e \tag{6}$$

For the boundary-layer system, we define a Lyapunov function $W(e) = e^{\mathrm{T}} P_0 e$, where P_0 is the symmetric positive definite solution of the Lyapunov function $A_0^{\mathrm{T}} P_0 + P_0 A_0 = -I$. Let $\lambda_{\min}$ and $\lambda_{\max}$ denote the minimum and maximum eigenvalues of P_0, respectively. Proposition 1 below is similar to Proposition 1 in [7] and result obtained in [19] and hence stated without proof.

Proposition 1

Consider the system of Eq. 1, for which Assumptions 1, 3 and 4 hold. If $x_0 := x(0) \in \Omega_b$, where $0 < b < c$, then given $b' \in (b, c)$, there exists a finite time t_e, independent of ε, such that $x(t) \in \Omega_{b'}$ for all $t \in [0, t_e]$. Furthermore, there exists $\sigma > 0$, independent of ε, such that for any $e(t) \in \mathcal{W}_o := \{e \in \mathbb{R}^n : W(e) \geq \sigma \varepsilon^2\}$ and $x(t) \in \Omega_c$, $\dot{W} \leq -\frac{1}{2\varepsilon}\|e\|^2$.

Theorem 1 formalizes the convergence property of observer design and stability of closed loop system in the presence of uncertainty.

Theorem 1. Consider the system of Eq. (1), for which Assumptions 1-4 hold, under a stabilizing control law u_c. Given any $0 < b < c$, $d > 0$, $d' > 0$ and $\bar{\theta}$, there exist $\Delta^*(\bar{\theta}) > 0$ and $\varepsilon^*(\bar{\theta}) > 0$ such that if $\Delta \in (0, \Delta^*(\bar{\theta})]$, $\varepsilon \in (0, \varepsilon^*(\bar{\theta})]$, and $x_0 \in \Omega_b$, then 1) there exists an integer $k' > 0$ such that $\|\hat{x}(t_k) - x(t_k)\| \leq d' \; \forall \; t_k \geq t_{k'}$, and 2) $x(t) \in \Omega_c \; \forall \; t \geq 0$ and $\limsup_{t \to \infty} \|x(t)\| \leq d$.

Proof

The proof is divided into two parts. In the first part, we establish that the scalded estimation error converges to a bounded region in a finite time. To this end, we show that given $e_b(\bar{\theta}) > 0$, which is

Prepared using rncauth.cls DOI: 10.1002/rnc

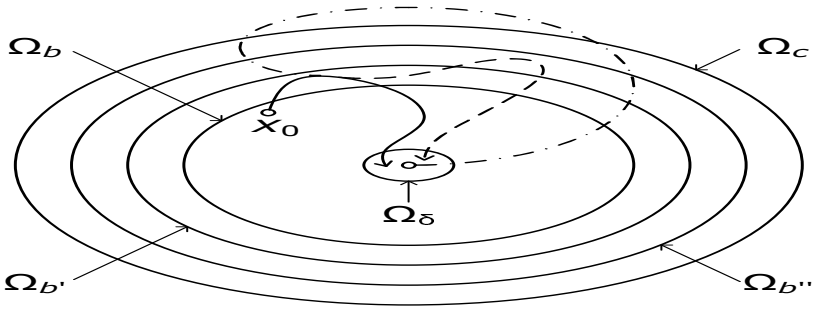

Figure 1. Schematic of the stability region, the evolution of the closed-loop state trajectories under fault-free (solid line) and faulty (dashed line) conditions, and the state estimate converging to its true value (dash-dotted line). The notation Ω_c denotes the stability region obtained under state feedback control ([7]).

to be determined in the second part, there exists $\varepsilon^* > 0$ such that if $\varepsilon \in (0, \varepsilon^*(\bar{\theta})]$ and $\Delta \in (0, t_e]$, then the scaled estimation error $e(t_k^-)$ enters $\mathcal{E} := \{e \in \mathbb{R}^n : \|e\| \leq e_b(\bar{\theta})\}$ no later than the time t_e defined in Proposition 1, and stays in $\mathcal{E}$ thereafter as long as $x(t)$ remains in Ω_c. In the second part of the proof, we show that boundedness of the scaled estimation error, e, guaranties boundedness of the estimation error, $\hat{x} - x$. To this end, we establish that for any $d > 0$ and $d' > 0$, there exists $e_b^* > 0$ and $\Delta^*(\bar{\theta}) > 0$ such that if $e(t_{k'}^-) \in \mathcal{E}$, $e_b \in (0, \min\{e_b^*(\bar{\theta}), \frac{d' - \bar{\theta}\Delta}{L_2}\}]$ where L_2 is a positive constant to be determined in the proof, and $\Delta \in (0, \Delta^*(\bar{\theta})]$, then $\|\hat{x}(t_k) - x(t_k)\| \leq d' \; \forall \; t_k \geq t_{k'}$, $x(t) \in \Omega_c$ $\forall \; t \geq t_{k'}$, and $\limsup_{t \to \infty} \|x(t)\| \leq d$ (see the solid line in Fig. 1).. Consider $\Delta \in (0, \Delta_1(\bar{\theta})]$ and $\varepsilon \in (0, \varepsilon_1(\bar{\theta})]$, where $\Delta_1(\bar{\theta}) = t_e$ and $\varepsilon_1(\bar{\theta}) = \sqrt{\frac{\gamma}{\sigma}}$, with $0 < \gamma < \min_{\|e\| = e_b} W(e)$. In order to show that $e(t_k^-)$ converges to $\mathcal{E}$, we only need to show that it converges to $\mathcal{W}_i := \{e \in \mathbb{R}^n : W(e) \leq \sigma\varepsilon^2\}$.

Part 1: We first show that $e(t_k^-)$ reaches $\mathcal{W}_i$ no later than the time t_e. Let N be the largest integer such that $N\Delta \leq t_e$. It follows from Proposition 1 that if $t_{k+1} \leq t_e$, $k = 0, \ldots, N-1$, then for any $e \in \mathcal{W}_o$ and $t \in [t_k, t_{k+1})$, we have

$$\dot{W} \leq -\frac{1}{2\lambda_{\max}\varepsilon} W \tag{7}$$

It follows that

$$W(e(t_{k+1}^-)) \leq e^{-\frac{\Delta}{2\lambda_{\max}\varepsilon}} W(e(t_k)) \tag{8}$$

Prepared using rncauth.cls
DOI: 10.1002/rnc

Let $\omega_{\max} = \max_{i=1,\ldots,p}\{\omega_i\}$. Since $T(x,u)$, $T'(x,u)$, $T^{-1}(\zeta,u)$ and $T'^{-1}(\zeta,u)$ are locally Lipschitz in x and ζ, respectively, and

$$\begin{aligned} e(t_k) &= D^{-1}[\zeta(t_k) - \hat{\zeta}(t_k)] = D^{-1}[T(x(t_k),u(t_k)) - T'(\hat{x}(t_k),u(t_k))] \\ &= D^{-1}[T'(x(t_k),u(t_k)) + T_\theta(x(t_k),u(t_k)) - T'(\hat{x}(t_k),u(t_k))] \end{aligned} \tag{9}$$

There exists $L_1, L_2 > 0$ such that the following equation holds:

$$\begin{aligned} \|e(t_k)\| &\le L_1 \max\{1,\varepsilon^{1-\omega_{\max}}\}\|x(t_k) - \hat{x}(t_k)\| + L_1 \max\{1,\varepsilon^{1-\omega_{\max}}\}T_{\bar{\theta}} \\ &= L_1 \max\{1,\varepsilon^{1-\omega_{\max}}\} \times \|T^{-1}(\zeta(t_{k-1}),u(t_{k-1})) - T'^{-1}(\hat{\zeta}(t_{k-1}),u(t_{k-1}))\| \\ &+ L_1 \max\{1,\varepsilon^{1-\omega_{\max}}\}T_{\bar{\theta}} \\ &= L_1 \max\{1,\varepsilon^{1-\omega_{\max}}\} \times \|T'^{-1}(\zeta(t_{k-1}),u(t_{k-1})) + T_{dev}^{-1}(\zeta(t_{k-1}),u(t_{k-1})) \\ &- T'^{-1}(\hat{\zeta}(t_{k-1}),u(t_{k-1}))\| + L_1 \max\{1,\varepsilon^{1-\omega_{\max}}\}T_{\bar{\theta}} \\ &\le L_1 \max\{1,\varepsilon^{1-\omega_{\max}}\} \times \|T'^{-1}(\zeta(t_{k-1}),u(t_{k-1})) - T'^{-1}(\hat{\zeta}(t_{k-1}),u(t_{k-1}))\| \\ &+ L_1 \max\{1,\varepsilon^{1-\omega_{\max}}\}\bar{T}_\theta + L_1 \max\{1,\varepsilon^{1-\omega_{\max}}\}\bar{\theta}\Delta \\ &= L_1 \max\{1,\varepsilon^{1-\omega_{\max}}\} \times \|T'^{-1}(\zeta(t_{k-1}),u(t_{k-1})) - T^{-1}(\hat{\zeta}(t_{k-1}),u(t_{k-1}))\| \\ &\le L_1 L_2 \max\{1,\varepsilon^{1-\omega_{\max}}\} \times \max\{1,\varepsilon^{\omega_{\max}-1}\}\|e(t_k^-)\| + L_1 \max\{1,\varepsilon^{1-\omega_{\max}}\}\bar{T}_\theta \\ &+ L_1 \max\{1,\varepsilon^{1-\omega_{\max}}\}\bar{\theta}\Delta = L_1 L_2 \beta_1(\varepsilon)\|e(t_k^-)\| + L_1\beta_1(\varepsilon)\bar{T}_\theta + L_1\beta_1(\varepsilon)\bar{\theta}\Delta \end{aligned} \tag{10}$$

where $\|T_\theta(x(t_k),u(t_k))\| \le \bar{T}_\theta$, $T_{dev}^{-1}(\zeta(t_{k-1}),u(t_{k-1})) = \int_{t_{k-1}}^{t_k} \theta(x,u,t)d\tau$ denotes the effect of the uncertainty on x with $\|T_{dev}^{-1}(\zeta(t_{k-1}),u(t_{k-1}))\| \le \bar{\theta}\Delta$ and $\beta_1(\varepsilon) = \varepsilon^{(\omega_{\max}-1)\mathrm{sgn}(\varepsilon-1)}$. Let $\tilde{L}_1 = L_1L_2$. It follows from Eqs. (8) and (10) that if $e(t) \in \mathcal{W}_o$ for all $t \in [t_k, t_{k+1})$, then the following

Prepared using rncauth.cls
DOI: 10.1002/rnc

equation holds:

$$\begin{aligned} W(e(t_{k+1})) &\leq \lambda_{\max}\|e(t_{k+1})\|^2 \\ &\leq \lambda_{\max}\tilde{L}_1^2[\beta_1(\varepsilon)]^2\|e(t_{k+1}^-)\|^2 + \lambda_{\max}L_1^2[\beta_1(\varepsilon)]^2\bar{T}_\theta^2 \\ &+ \lambda_{\max}L_1^2[\beta_1(\varepsilon)][\bar{\theta}\Delta]^2 + 2\lambda_{\max}\tilde{L}_1^2\beta_1(\varepsilon)\|e(t_k^-)\|L_1\beta_1(\varepsilon)\bar{T}_\theta \\ &+ 2\lambda_{\max}L_1^2\beta_1(\varepsilon)\|e(t_k^-)\|Ł_1\beta_1(\varepsilon)\bar{\theta}\Delta + 2\lambda_{\max}L_1\beta_1(\varepsilon)\bar{T}_\theta L_1\beta_1(\varepsilon)\bar{\theta}\Delta \\ &\leq \frac{\lambda_{\max}}{\lambda_{\min}}\tilde{L}_1^2[\beta_1(\varepsilon)]^2 e^{-\frac{\Delta}{2\lambda_{\max}\varepsilon}}W(e(t_k)) + \lambda_{\max}L_1^2[\beta_1(\varepsilon)]^2\bar{T}_\theta^2 \\ &+ \lambda_{\max}L_1^2[\beta_1(\varepsilon)][\bar{\theta}\Delta]^2 + 2\lambda_{\max}\tilde{L}_1^2L_1\beta_1^2(\varepsilon)\|e(t_k^-)\|\bar{T}_\theta \\ &+ 2\lambda_{\max}L_1^3\beta_1^2(\varepsilon)\|e(t_k^-)\|\,\bar{\theta}\Delta + 2\lambda_{\max}L_1^2\beta_1^2(\varepsilon)\bar{T}_\theta\bar{\theta}\Delta \end{aligned} \tag{11}$$

It follows form Eq. 7 that once $e(t)$ reaches $\mathcal{W}_i$, it stays there at least until the end of the same time interval. Since $T(x,u)$ is continuous, for any $x_0 \in \Omega_b$ and $\hat{x}_0 \in \mathcal{Q}$, there exists $K_1 > 0$ such that

$$\|e(0)\| \leq K_1\beta_2(\varepsilon) \tag{12}$$

where $\beta_2(\varepsilon) = \max\{1, \varepsilon^{1-\omega_{\max}}\}$ and as a result, using Eq. 10, we get

$$\begin{aligned} \|e(t_k)\| &\leq (\tilde{L}_1\beta_1(\varepsilon))^N(K_1\beta_2(\varepsilon))^N + (\tilde{L}_1\beta_1(\varepsilon))^{N-1}(L_1\beta_1(\varepsilon)\bar{T}_\theta + L_1\beta_1(\varepsilon)\bar{\theta}\Delta) \\ &+ (\tilde{L}_1\beta_1(\varepsilon))^{N-2}(L_1\beta_1(\varepsilon)\bar{T}_\theta + L_1\beta_1(\varepsilon)\bar{\theta}\Delta) + \ldots \\ &+ (L_1\beta_1(\varepsilon)\bar{T}_\theta + L_1\beta_1(\varepsilon)\bar{\theta}\Delta) \end{aligned} \tag{13}$$

To guarantee that $e(t_k^-)$ reaches $\mathcal{W}_i$ by the time t_N, it is required that the following equation hold:

$$\begin{aligned} &\frac{\lambda_{\max}}{\lambda_{\min}}\tilde{L}_1^2[\beta_1(\varepsilon)]^2 e^{-\frac{\Delta}{2\lambda_{\max}\varepsilon}}W(e(t_k)) + \lambda_{\max}L_1^2[\beta_1(\varepsilon)]^2\bar{T}_\theta^2 + \lambda_{\max}L_1^2[\beta_1(\varepsilon)]^2[\bar{\theta}\Delta]^2 \\ &+ 2\lambda_{\max}\tilde{L}_1^2L_1\beta_1^2(\varepsilon)\|e(t_k^-)\|\bar{T}_\theta + 2\lambda_{\max}L_1^3\beta_1^2(\varepsilon)\|e(t_k^-)\|\,\bar{\theta}\Delta \\ &+ 2\lambda_{\max}L_1^2\beta_1^2(\varepsilon)\bar{T}_\theta\bar{\theta}\Delta \leq \sigma\varepsilon^2 \end{aligned} \tag{14}$$

Using Eq. 13, we get

$$\begin{aligned} &\frac{\lambda_{\max}}{\lambda_{\min}}\tilde{L}_1^2[\beta_1(\varepsilon)]^2 e^{-\frac{\Delta}{2\lambda_{\max}\varepsilon}}W(e(t_k)) + \lambda_{\max}L_1^2[\beta_1(\varepsilon)]^2\bar{T}_\theta^2 + \lambda_{\max}L_1^2[\beta_1(\varepsilon)]^2[\bar{\theta}\Delta]^2 \\ &+ 2\lambda_{\max}\tilde{L}_1^2L_1\beta_1^2(\varepsilon)\|e(t_k^-)\|\bar{T}_\theta + 2\lambda_{\max}L_1^3\beta_1^2(\varepsilon)\|e(t_k^-)\|\,\bar{\theta}\Delta \\ &+ 2\lambda_{\max}L_1^2\beta_1^2(\varepsilon)\bar{T}_\theta\bar{\theta}\Delta \leq [\frac{\lambda_{\max}}{\lambda_{\min}}\tilde{L}_1^2[\beta_1(\varepsilon)]^2 e^{-\frac{\Delta}{2\lambda_{\max}\varepsilon}}]^N\lambda_{max}K_1^2[\beta_2(\varepsilon)]^2 \\ &+ \Gamma([\beta_1(\varepsilon)]^N[\beta_2(\varepsilon)]^N, [\beta_1(\varepsilon)]^s\bar{T}_\theta^q, [\beta_1(\varepsilon)]^n[\bar{\theta}\Delta]^z)^z) \end{aligned} \tag{15}$$

Prepared using rncauth.cls
DOI: 10.1002/rnc

where Γ is continuous in ε and $s \geq q$ and $n \geq z$. Therefore if the following inequality holds, then Eq. (14) holds too:

$$\begin{aligned} &\frac{\lambda_{\max}}{\lambda_{\min}} \tilde{L}_1^2 [\beta_1(\varepsilon)]^2 e^{-\frac{\Delta}{2\lambda_{\max}\varepsilon}}]^N \lambda_{max} K_1^2 [\beta_2(\varepsilon)]^2 \\ &+ \Gamma([\beta_1(\varepsilon)]^N [\beta_2(\varepsilon)]^N, [\beta_1(\varepsilon)]^s \bar{T}_\theta^q, [\beta_1(\varepsilon)]^n [\bar{\theta}\Delta]^z) \leq \sigma \end{aligned} \tag{16}$$

Rearranging the above equation gives

$$\begin{aligned} &\frac{1}{\varepsilon^2} \frac{\lambda_{\max}}{\lambda_{\min}} \tilde{L}_1^2 [\beta_1(\varepsilon)]^2 e^{-\frac{\Delta}{2\lambda_{\max}\varepsilon}}]^N \lambda_{max} K_1^2 [\beta_2(\varepsilon)]^2 \\ &+ \frac{1}{\varepsilon^2} \Gamma([\beta_1(\varepsilon)]^N [\beta_2(\varepsilon)]^N, [\beta_1(\varepsilon)]^s \bar{T}_\theta^q, [\beta_1(\varepsilon)]^n [\bar{\theta}\Delta]^z) \leq \sigma \end{aligned} \tag{17}$$

Since the left-hand side of the above inequality is continuous in ε and tends to zero as ε tends to 0, there exists $\varepsilon_2(\bar{\theta}) > 0$ such that if $\varepsilon \in (0, \varepsilon_2(\bar{\theta})]$, then Eq. (14) holds.

We then show that after the scaled estimate error $e(t_k^-)$ reaches $\mathcal{W}_i$, it stays there as long as $x(t)$ stays in Ω_c. Note that given $e(t_k^-) \in \mathcal{W}_i$, it is possible that $e(t_k)$ goes outside $\mathcal{W}_i$ due to the re-initialization to the system state and its estimate in the ζ coordinate. It follows from Eq. (10) that if $e(t_k^-) \in \mathcal{W}_i$, then $\|e(t_k)\| \leq \tilde{L}_1 \beta_1(\varepsilon) e_b + L_1 \beta_1(\varepsilon) \bar{T}_\theta + L_1 \beta_1(\varepsilon) \bar{\theta}\Delta$.

To guarantee that $e(t_{k+1}^-)$ stays in $\mathcal{W}_i$, it is required that the following equation hold:

$$e^{-\frac{\Delta}{2\lambda_{\max}\varepsilon}} \lambda_{\max} \tilde{L}_1^2 [\beta_1(\varepsilon)]^2 e_b^2 + L_1 \beta_1(\varepsilon) \bar{T}_\theta + L_1 \beta_1(\varepsilon) \bar{\theta}\Delta \leq \sigma\varepsilon^2 \tag{18}$$

It can be shown that there exists $\varepsilon_3(\bar{\theta}) > 0$ such that if $\varepsilon \in (0, \varepsilon_3(\bar{\theta})]$, then Eq. (18) holds.

Part 2: We first show that if the system state resides within a subset of Ω_c and the scaled estimation error is sufficiently small, then the state estimate also resides within Ω_c. It follows from the first part of the proof that we have

$$\begin{aligned} \|x - \hat{x}\| &= \|T^{-1}(\zeta, u) - T'^{-1}(\hat{\zeta}, u)\| = \|T'^{-1}(\zeta, u) + T_{dev}^{-1}(\zeta, u) - T'^{-1}(\hat{\zeta}, u)\| \\ &\leq L_2 \beta_3(\varepsilon) \|e\| + \bar{\theta}\Delta \leq L_2 \beta_3(\varepsilon_1) \|e\| + \bar{\theta}\Delta \end{aligned} \tag{19}$$

where $\beta_3(\varepsilon) = \max\{1, \varepsilon^{\omega_{\max}-1}\}$. It can be shown that given $0 < \delta_1 < \delta_2$, there exists $\tilde{e} > 0$ such that if $e_b \in (0, \tilde{e}]$, then $V(x) \leq \delta_1$ implies $V(\hat{x}) \leq \delta_2$. It follows from Proposition 1 that given $b' \in (b, c)$, we have that $x(t_{k'}) \in \Omega_{b'}$. Therefore, there exists $e_{b,1} > 0$ such that if $e_b \in (0, e_{b,1}(\bar{\theta})]$, then $\hat{x}(t_{k'}) \in \Omega_c$.

Prepared using rncauth.cls
DOI: 10.1002/rnc

We then show the existence of $e_b^*(\bar{\theta}) > 0$ and $\Delta^*(\bar{\theta}) > 0$ such that if $e_b \in (0, e_b^*(\bar{\theta})]$ and $\Delta \in (0, \Delta^*(\bar{\theta})]$, then any state trajectory originating in $\Omega_{b'}$ at time $t_{k'}$ converges to a closed ball of radius d around the origin. Since $V(x)$ is a continuous function of the state, one can find a positive real number $\delta < b'$ such that $V(x) \leq \delta$ implies $\|x\| \leq d$. Let $\hat{\delta}$ be a positive real number such that $0 < \hat{\delta} < \delta$. If $e_b \in (0, e_{b,1}(\bar{\theta})]$, the state estimate at time $t_{k'}$ can either be such that $\hat{\delta} < V(\hat{x}(t_{k'})) \leq c$ or $V(\hat{x}(t_{k'})) \leq \hat{\delta}$.

Case 1: Consider $\hat{x}(t_k) \in \Omega_c \backslash \Omega_{\hat{\delta}}$. Let $\dot{V}(x,u) = L_f V(x) + L_g V(x) u + L_\theta V(x)$. For this case, we have $\dot{V}(\hat{x}(t_k),\, u(t_k)) \leq -\alpha(V(\hat{x}(t_k))) < -\alpha(\hat{\delta})$. It follows from the continuity properties of $f(\cdot)$, $g(\cdot)$, $\theta(\cdot)$ and $V(\cdot)$ that $L_f V(\cdot)$, $L_g V(\cdot)$ and $L_\theta V(\cdot)$ are locally Lipschitz on the domain of interest. Therefore, there exists $L_3 > 0$ such that

$$|\dot{V}(x(t_k), u(t_k)) - \dot{V}(\hat{x}(t_k), u(t_k))| \leq L_3 \|x(t_k) - \hat{x}(t_k)\| \leq L_2 L_3 \beta_3(\varepsilon_1) \|e(t_k^-)\| + L_3 \bar{\theta} \Delta \tag{20}$$

Since the functions $f(\cdot)$, $g(\cdot)$ and $\theta(\cdot)$ are continuous, u is bounded, and $\Omega_{b'}$ is bounded, one can find $K_2 > 0$ such that $\|x(t) - x(t_k)\| \leq K_2 \Delta$ for any $\Delta \in (0, \Delta_1]$, $x(t_k) \in \Omega_{b'}$ and $t \in [t_k, t_k + \Delta)$. It follows that $\forall\, t \in [t_k, t_k + \Delta)$, the following equation holds:

$$\begin{aligned} \dot{V}(x(t)) &= \dot{V}(\hat{x}(t_k), u(t_k)) + [\dot{V}(x(t), u(t_k)) - \dot{V}(x(t_k), u(t_k)] \\ &\quad + [\dot{V}(x(t_k), u(t_k)) - \dot{V}(\hat{x}(t_k), u(t_k))] \\ &< -\alpha(\hat{\delta}) + L_3 K_2 \Delta + L_2 L_3 \beta_3(\varepsilon_1(\bar{\theta})) \|e(t_k^-)\| + L_3 \bar{\theta} \Delta \end{aligned} \tag{21}$$

Consider $\Delta \in (0, \Delta_2(\bar{\theta})]$, where $\Delta_2 = \frac{\alpha(\hat{\delta})}{3 L_3 K_2}$, and $e_b \in (0, e_{b,2}(\bar{\theta})]$, where $e_{b,2}(\bar{\theta}) = \frac{\alpha(\hat{\delta}) - L_3 \bar{\theta} \Delta}{3 L_2 L_3 \beta_3(\varepsilon_1(\bar{\theta}))}$. Then, we have

$$\dot{V}(x(t)) < -\frac{1}{3} \alpha(\hat{\delta}) < 0 \tag{22}$$

Since $\dot{V}(x(t))$ remains negative over $[t_k, t_k + \Delta)$, $x(t)$ remains in Ω_c over the same time interval, and $V(x(t_k + \Delta)) < V(x(t_k))$.

If $\hat{x}(t_{k'}) \in \Omega_c \backslash \Omega_{\hat{\delta}}$, we have $\dot{V}(x(t)) < 0$ over $[t_{k'}, t_{k'} + \Delta)$. It follows that $\hat{x}(t_{k'+1}) \in \Omega_c$ for $e_b \in (0, e_{b,1}(\bar{\theta})]$. Similarly, it can be shown that for $t_k > t_{k'}$, $\dot{V}(x(t))$ remains negative until $\hat{x}(t_k)$ reaches $\Omega_{\hat{\delta}}$.

Prepared using rncauth.cls
DOI: 10.1002/rnc

Case 2: Consider $\hat{x}(t_k) \in \Omega_{\hat{\delta}}$. For this case, it is established in the proof of the second part of Theorem 1 in [7], that there exist $e_{b,3}(\bar{\theta}) > 0$ and $\Delta_3(\bar{\theta}) > 0$ such that if $e_b \in (0, e_{b,3}(\bar{\theta})]$ and $\Delta \in (0, \Delta_3(\bar{\theta})]$, we have $x(t_{k+1}) \in \Omega_\delta$ and as a result $\hat{x}(t_{k+1}) \in \Omega_c$ for $e_b \in (0, e_{b,1}(\bar{\theta})])$.

For $e_b \in (0, e_b^*(\bar{\theta})]$ and $\Delta \in (0, \Delta^*(\bar{\theta})]$, where $e_b^* = \min\{e_{b,1}(\bar{\theta}), e_{b,2}(\bar{\theta}), e_{b,3}(\bar{\theta})\}$ and $\Delta^*(\bar{\theta}) = \min\{\Delta_1(\bar{\theta}), \Delta_2(\bar{\theta}), \Delta_3(\bar{\theta})\}$, it can be shown by iteration that any state trajectory originating in $\Omega_{b'}$ at time $t_{k'}$ converges to the set Ω_δ, and hence converges to the closed ball of radius d around the origin. Furthermore, if $e_b \leq \frac{d' - \bar{\theta}\Delta}{L_2}$, it follows from Eq. (19) that $\|\hat{x}(t_k) - x(t_k)\| \leq d' \; \forall \; t_k \geq t_{k'}$.

In summary, it is established that given any $0 < b < c$, $d > 0$ and $d' > 0$, there exist $\Delta^*(\bar{\theta}) > 0$ and $\varepsilon^*(\bar{\theta}) > 0$ such that if $\Delta \in (0, \Delta^*(\bar{\theta})]$, $\varepsilon \in (0, \varepsilon^*(\bar{\theta})]$, and $x_0 \in \Omega_b$, then 1) $\|\hat{x}(t_k) - x(t_k)\| \leq d'$ $\forall \; t_k \geq t_{k'}$, and 2) $x(t) \in \Omega_c \; \forall \; t \geq 0$ and $\limsup_{t \to \infty} \|x(t)\| \leq d$. This concludes the proof of Theorem 1. □

4. FAULT DETECTION AND ISOLATION MECHANISM

In this section, we now present the fault detection and isolation mechanism. Considering scenarios where at most two, actuator and/or sensor, experiences a faults. This leads to $m + \frac{m(m-1)}{2} + p + \frac{p(p-1)}{2} + mp$ unique scenarios. Residuals (with the associated high gain observers) are designed for each fault scenario in the same fashion as [6].

Specifically, the residuals for a fault scenario are defined as the norm of the difference between the state prediction and the state estimate for the subsystem model that does not require the value of the corresponding actuator/sensor in the calculations (see [6] for more details). Each residual is designed in a way that is only insensitive to the specific fault scenario but sensitive to the other fault scenario. To this end, let $\Theta_{f,i}$ denote the fault vector (sensor/and or actuator) for the ith fault scenario, and $\bar{\Theta}_{f,i}$ the remaining fault variable vector (the remaining u_f and y_f variables). Specifically, let $u_{f,i}$ and $y_{f,i}$ denote the vectors of input and output variables subject to faults $\Theta_{f,i}$, respectively. Let $\bar{u}_{f,i}$ and $\bar{y}_{f,i}$ denote the vectors of the rest of the input and output variables, respectively.

Prepared using rncauth.cls
DOI: 10.1002/rnc

Assumption 5

[6] Assumptions 1 and 2 in hold for the system of Eq. (1), with $\bar{u}_{f,i}$ and $\bar{y}_{f,i}$ being the vectors of input and output variables, respectively, $i = 1, \ldots, n_f$.

Under Assumption 5, the state observer for the ith fault scenario is designed as follow :

$$\begin{aligned} \dot{\hat{\zeta}}^j &= A^j \hat{\zeta}^j + H^j(\bar{y}_{f,i} - C^j \hat{\zeta}^j) \\ \dot{\hat{\zeta}}^j(t_k) &= T'^j(\hat{x}^j(t_k), \bar{u}_{f,i}(t_k)) \end{aligned} \tag{23}$$

where j presents the jth observer with $j = 1, \ldots, p + \frac{p(p-1)}{2}$. To define residuals, we need to compute expected trajectories. To this end, we consider a subsystem of Eq. 1 for which the state variables are all of those such that no inputs in u_{f_i} appear on the right-hand side of the corresponding ODE's. Let x_{sub} denote the vector of state variables for the subsystem, and $\bar{x}_{sub,}$ the vector of the rest of the state variables. Without loss of generality, the model of the subsystem can be described as follows:

$$\begin{aligned} \dot{x}_{sub,i} = f_{sub,i}([x_{sub,i}^{\mathrm{T}}, \bar{x}_{sub,i}^{\mathrm{T}}]^{\mathrm{T}}) + G_{sub,i}([x_{sub,i}^{\mathrm{T}}, \bar{x}_{sub,i}^{\mathrm{T}}]^{\mathrm{T}})\bar{u}_{f,i} \\ + \theta_{sub,i}([x_{sub,i}^{\mathrm{T}}, \bar{x}_{sub,i}^{\mathrm{T}}]^{\mathrm{T}}, \bar{u}_{f,i}, t) \end{aligned} \tag{24}$$

where $f_{sub,i}(\cdot)$, $G_{sub,i}(\cdot)$ and $\theta_{sub,i}(\cdot)$ are appropriately defined. For each faulty scenario, the expected system trajectory is computed using the known part of the system model and the state estimates generated by the jth observer that does not require values of the variables included in the fault vector $\Theta_{f,i}$. Specifically, for $t \in [t_{k-T}, t_k)$, a prediction model is designed as follows:

$$\dot{\tilde{x}}_{sub,i,j} = f_{sub,i}([\tilde{x}_{sub,i,j}^{\mathrm{T}}, \hat{\bar{x}}_{sub,i,j}^{\mathrm{T}}]^{\mathrm{T}}) + G_{sub,i}([\tilde{x}_{sub,i,j}^{\mathrm{T}}, \hat{\bar{x}}_{sub,i,j}^{\mathrm{T}}]^{\mathrm{T}})\bar{u}_{f,i} \tag{25}$$

where $\tilde{x}_{sub,i,j}$ is the state of the prediction model, $\hat{\bar{x}}_{sub,i,j}$ is the estimate of $\bar{x}_{sub,i}$ provided by the jth observer, and T is the prediction horizon: $T = 1$ if $0 < t_k \leq t_{k'}$; $T = k - k'$ if $t_{k'} < t_k \leq t_{k'+T_p}$; and $T = T_p$ if $t_k > t_{k'+T_p}$, with a positive integer T_p being a chosen prediction horizon. The initial condition for the prediction model is the state estimate at time t_{k-T}: $\tilde{x}_{sub,i,j}(t_{k-T}) = \hat{x}_{sub,i,j}(t_{k-T})$. Let $\tilde{x}_{sub,i,j}(t_k)$ denote the prediction for the state vector $x_{sub,i}$ at time t_k. By solving Eq. (25), the state prediction at time t_k is obtained.

The residuals are defined as the norm of the difference between the state prediction and the state estimate for the subsystem that is not subject to faulty input (see e.g. [6]). For the ith faulty scenario,

Prepared using rncauth.cls
DOI: 10.1002/rnc

the residual (at the time instance t_{k+1}) is defined as follows:

$$r_{i,k+1} = \|\tilde{x}_{sub,i,j}(t_{k+1}) - \hat{x}_{sub,i,j}(t_{k+1})\| \tag{26}$$

Remark 4. Note that for defining the corresponding insensitive residuals to actuator faults, the prediction model utilizes the state measurements, if they are available. If not, they must be replaced by state estimates computed by the observer that does not require knowledge of the prescribed input. For defining the corresponding insensitive residuals to simultaneous actuator and a particular sensor faults, the specific sensor measurements can no longer be used in the prediction model and they are replaced by state estimates generated by an observer that does not use the prescribed input nor the specific sensor measurement. This is the key feature that enables us to distinguish between actuator faults and simultaneous actuator and sensor faults, in the absence of uncertainty.

Now we specify how the thresholds for the residuals need to be selected to enable FDI. Before proceeding to define thresholds corresponding to each residual, we need the following result presented as Lemma 1:

Lemma 1

Consider the system of Eq. 1, for which Assumptions 1-5 hold and residuals for each sample time are defined as in Eq. 26. Then under fault free condition, for $t_k \geq t_{k'}$ (see Theorem 1 for definition of k'):

$$r_{i,k+1} \leq L_{2,sub,i,j}\beta_2^i(\varepsilon)E_{s,sub,i,j} + \bar{\theta}_{sub,i}\Delta + E_p^i \tag{27}$$

where $E_{s,sub,i,j} = e^{-\alpha_{sub,i,j}\Delta}e_b^{*,i} + K_{B,sub,i,j}^i K_{\phi,,sub,i,j}^i \frac{1-e^{-\alpha_{sub,i,j}\Delta}}{\alpha_{sub,i,j}} + \frac{1-e^{-\alpha_{sub,i,j}\Delta}}{\alpha_{sub,i,j}}\bar{\eta}_{sub,i,j}$, sub and j refer to the corresponding subsystem and observer used for defining r_i, respectively, where i refers to ith residual, $e_b^{*,i}$ is the upper bound on $\|e_{sub,i,j}^i(t_k)\|$, K_B is spectrum bound of the matrix $\|B^i\|$, α is the spectrum bound of the matrix $\frac{A_0^i}{\varepsilon}$ and $E_p^i = M^i\Delta + K_{\tilde{e}}$, $\|(\tilde{f}_{sub,i} - f_{sub,i}([x_{sub,i}^{\mathrm{T}}, \bar{x}_{sub,i}^{\mathrm{T}}]^{\mathrm{T}})) + (\tilde{G}_{sub,i} - G_{sub,i}([x_{sub,i}^{\mathrm{T}}, \bar{x}_{sub,i}^{\mathrm{T}}]^{\mathrm{T}}))\bar{u}_{f,i}\| + \bar{\theta}_{sub,i} \leq M^i$,

where $\tilde{f}_{sub,i} = f_{sub,i}([\tilde{x}_{sub,i,j}^{\mathrm{T}}, \hat{\tilde{x}}_{sub,i,j}^{\mathrm{T}}]^{\mathrm{T}})$, $\tilde{G}_{sub,i} = G_{sub,i}([\tilde{x}_{sub,i,j}^{\mathrm{T}}, \hat{\tilde{x}}_{sub,i,j}^{\mathrm{T}}]^{\mathrm{T}})$, $K_{\tilde{e}}$ is the upper bound on $\|\tilde{e}_{i,k}(t_k)\|$ which is constant, where $\tilde{e}_{i,k} = \tilde{x}_{sub,i,j} - x_{sub,i}$ and $\tilde{x}_{sub,i,j}$ is state of prediction model defined in [6].

Prepared using rncauth.cls
DOI: 10.1002/rnc

Proof

By using triangular inequality, Eq. 26 turns to the following form:

$$\begin{aligned} r_{i,k+1} &= \|\tilde{x}_{sub,i,j}(t_{k+1}) - \hat{x}_{sub,i,j}(t_{k+1})\| \\ &\leq \|\tilde{x}_{sub,i,j}(t_{k+1}) - x_{sub,i}(t_{k+1})\| + \|x_{sub,i}(t_{k+1}) - \hat{x}_{sub,i,j}(t_{k+1})\| \\ &\leq \sup \|\tilde{x}_{sub,i,j}(t_{k+1}) - x_{sub,i}(t_{k+1})\| + \sup \|x_{sub,i}(t_{k+1}) - \hat{x}_{sub,i,j}(t_{k+1})\| \end{aligned} \tag{28}$$

Consider the prediction model corresponding to fault Θ_{f_i}:

$$\dot{\tilde{x}}_{sub,i,j} = f_{sub,i}([\tilde{x}^{\mathrm{T}}_{sub,i,j}, \hat{\tilde{x}}^{\mathrm{T}}_{sub,i,j}]^{\mathrm{T}}) + G_{sub,i}([\tilde{x}^{\mathrm{T}}_{sub,i,j}, \hat{\tilde{x}}^{\mathrm{T}}_{sub,i,j}]^{\mathrm{T}})\bar{u}_{f,i} \tag{29}$$

where $\tilde{x}_{sub,i,j}$ is the state of the prediction model, $\hat{\tilde{x}}_{sub,i,j}$ is the estimate of $\bar{x}_{sub,i}$ provided by the corresponding observer.

Defining $\tilde{e}_{i,k} = \tilde{x}_{sub,i,j} - x_{sub,i}$, we obtain:

$$\begin{aligned} \dot{\tilde{e}}_{i,k} = {} & f_{sub,i}([\tilde{x}^{\mathrm{T}}_{sub,i,j}, \hat{\tilde{x}}^{\mathrm{T}}_{sub,i,j}]^{\mathrm{T}}) - f_{sub,i}([x^{\mathrm{T}}_{sub,i}, \bar{x}^{\mathrm{T}}_{sub,i}]^{\mathrm{T}}) + \\ & (G_{sub,i}([\tilde{x}^{\mathrm{T}}_{sub,i,j}, \hat{\tilde{x}}^{\mathrm{T}}_{sub,i,j}]^{\mathrm{T}}) - G_{sub,i}([x^{\mathrm{T}}_{sub,i}, \bar{x}^{\mathrm{T}}_{sub,i}]^{\mathrm{T}}))\bar{u}_{f,i} \\ & - \theta_{sub,i}([x^{\mathrm{T}}_{sub,i}, \bar{x}^{\mathrm{T}}_{sub,i}]^{\mathrm{T}}, \bar{u}_{f,i}, t) \end{aligned} \tag{30}$$

For sake of brevity, we define $\tilde{f}_{sub,i} = f_{sub,i}([\tilde{x}^{\mathrm{T}}_{sub,i,j}, \hat{\tilde{x}}^{\mathrm{T}}_{sub,i,j}]^{\mathrm{T}})$, $\tilde{G}_{sub,i} = G_{sub,i}([\tilde{x}^{\mathrm{T}}_{sub,i,j}, \hat{\tilde{x}}^{\mathrm{T}}_{sub,i,j}]^{\mathrm{T}})$. By integration, we get:

$$\begin{aligned} \tilde{e}_{i,k}(t_{k+1}) = {} & \int_{t_k}^{t_{k+1}} (\tilde{f}_{sub,i} - f_{sub,i}([x^{\mathrm{T}}_{sub,i}, \bar{x}^{\mathrm{T}}_{sub,i}]^{\mathrm{T}}))d\tau + \int_{t_k}^{t_{k+1}} (\tilde{G}_{sub,i} - G_{sub,i}([x^{\mathrm{T}}_{sub,i}, \bar{x}^{\mathrm{T}}_{sub,i}]^{\mathrm{T}}))\bar{u}_{f,i} \\ & - \theta_{sub,i})d\tau + \tilde{e}_{i,k}(t_k) \end{aligned} \tag{31}$$

Under Assumptions 3 and 4 and by applying the triangular inequality, we obtain:

$$\begin{aligned} \|\tilde{e}_{i,k}(t_{k+1})\| \leq {} & \int_{t_k}^{t_{k+1}} \|(\tilde{f}_{sub,i} - f_{sub,i}([x^{\mathrm{T}}_{sub,i}, \bar{x}^{\mathrm{T}}_{sub,i}]^{\mathrm{T}}))\|d\tau + \int_{t_k}^{t_{k+1}} (\|(\tilde{G}_{sub,i} - G_{sub,i}([x^{\mathrm{T}}_{sub,i}, \bar{x}^{\mathrm{T}}_{sub,i}]^{\mathrm{T}})) \\ & \bar{u}_{f,i}\| + \|\theta_{sub,i}\|)d\tau + \|\tilde{e}_{i,k}(t_k)\| \leq M^i\Delta + K_{\tilde{e}} \end{aligned} \tag{32}$$

where $\|(\tilde{f}_{sub,i} - f_{sub,i}([x^{\mathrm{T}}_{sub,i}, \bar{x}^{\mathrm{T}}_{sub,i}]^{\mathrm{T}}))\| + \|(\tilde{G}_{sub,i} - G_{sub,i}([x^{\mathrm{T}}_{sub,i}, \bar{x}^{\mathrm{T}}_{sub,i}]^{\mathrm{T}}))\bar{u}_{f,i}\| + \bar{\theta}_{sub,i} \leq M^i$ and $\|\tilde{e}_{i,k}(t_k)\| \leq K_{\tilde{e}}$.

Prepared using rncauth.cls
DOI: 10.1002/rnc

Now we need to determine the supremum for $\|x_{sub,i}(t_{k+1}) - \hat{x}_{sub,i,j}(t_{k+1})\|$. For $t \in [t_k, t_{k+1})$, the scaled estimation error corresponding to ith residual evolves as follows:

$$\dot{e^i} = \frac{1}{\varepsilon^i} A_0^i e^i + B^i(\phi^i(\bar{u}_{f_i}) - \phi_0^i(\bar{u}_{f_i})) + \eta_i \tag{33}$$

The solution to the above equation gives

$$\begin{aligned} e^i(t_{k+1}) = &\int_{t_k}^{t_{k+1}} e^{\frac{A_0^i}{\varepsilon}(t_{k+1}-\tau)}[B^i(\phi^i(\zeta, \bar{u}_{f_i}, t) - \phi_0^i(\hat{\zeta}, \bar{u}_{f_i}, t)) + \eta_i(\zeta, u, t)]d\tau \\ &+ e^{-\frac{A_0^i}{\varepsilon}(t_k - t_{k+1})} e^i(t_k) \end{aligned} \tag{34}$$

Under Assumptions 3 and 4 and by applying the triangular inequality, we obtain:

$$\begin{aligned} \|e^i(t_{k+1})\| &\leq \| \int_{t_k}^{t_{k+1}} e^{\frac{A_0^i}{\varepsilon}(t_{k+1}-\tau)}[B^i(\phi^i(\zeta, \bar{u}_{f_i}, t) - \phi_0^i(\hat{\zeta}, \bar{u}_{f_i}, t)) + \eta_i(\zeta, u, t)]d\tau\| \\ &+ \|e^{-\frac{A_0^i}{\varepsilon}(t_k - t_{k+1})} e^i(t_k)\| \\ &\leq \| \int_{t_k}^{t_{k+1}} e^{\frac{A_0^i}{\varepsilon}(t_{k+1}-\tau)}[B^i(\phi^i(\zeta, \bar{u}_{f_i}, t) - \phi_0^i(\hat{\zeta}, \bar{u}_{f_i}, t))]d\tau\| \\ &+ \| \int_{t_k}^{t_{k+1}} e^{\frac{A_0^i}{\varepsilon}(t_{k+1}-\tau)}\eta_i(\zeta, u, t)]d\tau\| + \|e^{-\frac{A_0^i}{\varepsilon}(t_k - t_{k+1})} e^i(t_k)\| \\ &\leq \int_{t_k}^{t_{k+1}} e^{\frac{A_0^i}{\varepsilon}(t_{k+1}-\tau)}\|B^i\|\|(\phi^i(\zeta, \bar{u}_{f_i}, t) - \phi_0^i(\hat{\zeta}, \bar{u}_{f_i}, t))\|d\tau \\ &+ \int_{t_k}^{t_{k+1}} e^{\frac{A_0^i}{\varepsilon}(t_{k+1}-\tau)}\|\eta_i(\zeta, u, t)\|d\tau + e^{-\frac{A_0^i}{\varepsilon}(t_k - t_{k+1})}\|e^i(t_k)\| \\ &\leq e^{-\alpha\Delta} e_b^{*,i} + K_{B_i} K_{\phi_i} \frac{1 - e^{-\alpha_i \Delta}}{\alpha_i} + \frac{1 - e^{-\alpha_i \Delta}}{\alpha_i} \bar{\eta}_i \end{aligned} \tag{35}$$

where α_i, K_{B_i}, K_ϕ are the spectrum bound of the matrices $\frac{A_0^i}{\varepsilon}$, B^i, $(\phi^i(\zeta, \bar{u}_{f_i}, t) - \phi_0^i(\hat{\zeta}, \bar{u}_{f_i}, t))$ respectively, and $e_b^{*,i}$ is the upper bound on $\|e^i(t_k)\|$. From 19, we have

$$\|x - \hat{x}\| = \|T^{-1}(\zeta, u) - T'^{-1}(\hat{\zeta}, u)\| \leq L_2 \beta_3(\varepsilon) E_s + \bar{\theta}\Delta \tag{36}$$

where $\beta_2(\varepsilon) = \max\{1, \varepsilon^{\omega_{\max}-1}\}$, $L_2 > 0$, $E_s = e^{-\alpha\Delta} e_b^{*,i} + K_{B_i} K_{\phi_i} \frac{1-e^{-\alpha_i\Delta}}{\alpha_i} + \frac{1-e^{-\alpha_i\Delta}}{\alpha_i}\bar{\eta}_i$ and as a result,

$$\|x_{sub,i} - \hat{x}_{sub,i,j}\| \leq L_{2,sub,i,j} \beta_2(\varepsilon) E_{s,sub,i,j} + \bar{\theta}_{sub,i}\Delta \tag{37}$$

where $E_{s,sub,i,j} = e^{-\alpha_{sub,i,j}\Delta}\|e^i_{sub,i,j}(t_k)\|$

$+ K_{B,sub,i,j} K_{\phi,,sub,i,j} \frac{1-e^{-\alpha_{sub,i,j}\Delta}}{\alpha_{sub,i,j}} + \frac{1-e^{-\alpha_{sub,i,j}\Delta}}{\alpha_{sub,i,j}} \bar{\eta}_{sub,i,j}$. Using Eq. 32 and 36, $r_{i,k+1}$ is bounded

Prepared using rncauth.cls DOI: 10.1002/rnc

as below:

$$\begin{aligned} r_{i,k+1} &= \|\tilde{x}_{sub,i,j}(t_{k+1}) - \hat{x}_{sub,i,j}(t_{k+1})\| \\ &\leq \|\tilde{x}_{sub,i,j}(t_{k+1}) - x_{sub,i}(t_{k+1})\| + \|x_{sub,i}(t_{k+1}) - \hat{x}_{sub,i,j}(t_{k+1})\| \\ &\leq \sup \|\tilde{x}_{sub,i,j}(t_{k+1}) - x_{sub,i}(t_{k+1})\| + \sup \|x_{sub,i}(t_{k+1}) - \hat{x}_{sub,i,j}(t_{k+1})\| \\ &= L_{2,sub,i,j}\beta_2(\varepsilon)E_{s,sub,i,j} + \bar{\theta}_{sub,l}\Delta + E_p^i \end{aligned} \tag{38}$$

where $E_p = M^i\Delta + K_{\tilde{e}}$. This concludes proof of Lemma 1. □

Picking the threshold corresponding to each residual as below:

$$\delta_i = L_{2,sub,i,j}\beta_2(\varepsilon)E_{s,sub,i,j} + \bar{\theta}_{sub,l}\Delta + E_p^i \tag{39}$$

It follows from Lemma 1 then that under fault free condition $r_{i,k+1} \leq \delta_i$.

Remark 5. Note that the threshold defined by Eq. 39 depends on the observer gain, H, since α represents spectrum bound of $\frac{A_0^i}{\varepsilon}$ which is defined based on the observer gain. Therefore by changing the observer gain, the threshold value changes. The threshold values obtained by using Eq. 39 are constant since they are defined based on bound of the estimation error after convergence to stability region and a constant bound for the uncertainty. In contrast, the time-varying thresholds in [13] and [14] are due to considering the estimation error before converging to stability region in defining thresholds. Note that the thresholds defined in this work can be readily made time-varying by considering the estimation error before its convergence to stability region in defining thresholds. Also in the scenario that time-varying bounds for the uncertainty are known, the level of conservatism in thresholds can be further reduced.

A fault is detected when at least one of the residuals breach their threshold i.e. $r_{i,d} > \delta_i$, and we denote this time as t_d. It follows from Lemma 1 that there will be no false alarm before fault occurrence. Corollary 1 establishes that a residual designed to be insensitive to a specific fault scenario (using the approach in [6]) will remain insensitive even in the presence of uncertainty when thresholds are picked using the proposed approach. To this end, let r_{ins}^i denote the vector of insensitive residuals corresponding to the ith fault scenario, Θ_{f_i}.

Prepared using rncauth.cls
DOI: 10.1002/rnc

Corollary 1

Consider the system of Eq. 1, for which Assumptions 1-5 hold and the fault detection and isolation framework characterized by residuals and thresholds described by Eq. 26 and Eq. 39, respectively. The vector of insensitive residuals r^i_{ins} do not breach their corresponding thresholds when $\Theta_{f,i}(t) \neq 0$ i.e., for each $r_o \in r^i_{ins}$, $r_o \leq \delta_i \; \forall \; t > t_f \geq t_{k'}$.

Proof

Consider the system of Eq. 1 under fault free conditions and let $r_o \in r^i_{ins}$. From Lemma 1 for $t < t_f$, we have:

$$r_o = \|\tilde{x}_{sub,o,j} - \hat{x}_{sub,o,j}\| \leq \delta_o = r^o_{pp} + r^o_{ep} \tag{40}$$

where

$$\|\tilde{x}_{sub,o,j} - x_{sub,o,j}\| \leq r^o_{pp} = M^o\Delta + K_{\tilde{e}} \tag{41}$$

and

$$\|x_{sub,o,j} - \hat{x}_{sub,o,j}\| \leq r^o_{ep} = L_{2,sub,o,j}\beta_2(\varepsilon)E_{s,sub,o,j} + \bar{\theta}_{sub,o}\Delta \tag{42}$$

Now we show that for $t > t_f$ $\|\tilde{x}_{sub,o,j} - x_{sub,o,j}\| \leq r^o_{pp}(\bar{\theta}_{sub}, t)$ and $\|x_{sub,o,j} - \hat{x}_{sub,o,j}\| \leq r^o_{ep}(\bar{\theta}_{sub}, t)$. Since the governing equation of scaled estimation error corresponding to r_0 after fault occurrence is same as fault free condition:

$$\dot{e^o} = \frac{1}{\varepsilon^o}A^o_0 e^o + B^o(\phi^o(\bar{u}_f) - \phi^o_0(\bar{u}_f)) + \eta_o \tag{43}$$

Thus, for any arbitrarily sampling time after fault occurrence, Eq. 42 still holds.

After fault occurrence, $\tilde{x}_{sub,o,j}$ evolves as follows:

$$\dot{\tilde{x}}_{sub,o,j} = f_{sub,o}([\tilde{x}^{\mathrm{T}}_{sub,o,j}, \hat{\tilde{x}}^{\mathrm{T}}_{sub,o,j}]^{\mathrm{T}}) + G_{sub,o}([\tilde{x}^{\mathrm{T}}_{sub,i,j}, \hat{\tilde{x}}^{\mathrm{T}}_{sub,o,j}]^{\mathrm{T}})\bar{u}_{f,i} \tag{44}$$

It follows from Eq. 44 that the governing equation of $\tilde{e}_{o,k} = \tilde{x}_{sub,o,j} - x_{sub,o}$ is the same as fault free condition:

$$\dot{\tilde{e}}_{o,k} = f_{sub,o}([\tilde{x}^{\mathrm{T}}_{sub,o,j}, \hat{\tilde{x}}^{\mathrm{T}}_{sub,o,j}]^{\mathrm{T}}) - f_{sub,o}([x^{\mathrm{T}}_{sub,o}, \bar{x}^{\mathrm{T}}_{sub,i}]^{\mathrm{T}}) +$$
$$(G_{sub,o}([\tilde{x}^{\mathrm{T}}_{sub,o,j}, \hat{\tilde{x}}^{\mathrm{T}}_{sub,o,j}]^{\mathrm{T}}) - G_{sub,o}([x^{\mathrm{T}}_{sub,o}, \bar{x}^{\mathrm{T}}_{sub,i}]^{\mathrm{T}}))\bar{u}_{f,i} - \theta_{sub,i}([x^{\mathrm{T}}_{sub,o}, \bar{x}^{\mathrm{T}}_{sub,o}]^{\mathrm{T}}, \bar{u}_{f,i}, t) \tag{45}$$

Prepared using rncauth.cls
DOI: 10.1002/rnc

And as a result, for $t > t_f$, $\|\tilde{x}_{sub,i,j} - x_{sub,i,j}\| \leq r^o_{pp}(\bar{\theta}_{sub}, t)$. This concludes the proof of Corollary 1. □

Detectability Analysis for Simultaneous Actuator and Sensor Faults

In this section, we establish the conditions necessary for the sensitive residuals to breach their thresholds in the presence of uncertainty via a detectability analysis (see e.g, [14], [20], [21], [22], [23], [24] and [25]). Theorem 2 presents the sufficient conditions for simultaneous single actuator and single sensor faults to be detectable by the proposed FDI framework. To this end, let $r_{\bar{u}_{f_i},\bar{y}_{f_i}}$ denote a sensitive residual to simultaneous faults u_{f_i} and y_{f_i} defined as:

$$r_{\bar{u}_{f_i},\bar{y}_{f_i},k+1} = \|\tilde{x}_{sub,\bar{u}_{f_i},\bar{y}_{f_i}}(t_{k+1}) - \hat{x}_{sub,\bar{u}_{f_i},\bar{y}_{f_i}}(t_{k+1})\| \tag{46}$$

Theorem 2. Consider the system of Eq. 1, for which Assumptions 1-5 hold and the fault detection and isolation framework characterized by residual and threshold described by Eq. 26 and Eq. 39, respectively. When single actuator u_{f_i} and single sensor fault y_{f_i} occur simultaneously at time t_f: If there exists an interval of time $[t_f, t_d]$ where $t_f \geq t_{k'}$, such that the fault functions u_{f_i} and y_{f_i} satisfy

$$\begin{aligned}&\|\frac{1}{L'_{2,u_i}\beta_2(\varepsilon)}\|\vartheta(\frac{A_{0,sub,i,j}}{\varepsilon}, H_{sub,\bar{u}_{f_i},\bar{y}_{f_i}}, y_{f_i})\| + \|Dev_{t_f\ldots t_d}(\tilde{x}^{\mathrm{T}}_{sub,\bar{u}_{f_i},\bar{y}_{f_i}}, \bar{u}_{f_i}, f_d, x^{\mathrm{T}}_{sub,\bar{u}_{f_i},\bar{y}_{f_i}}, u_{f_i})\| \\ &+ \|f_{d,u_{f_i}}\| - \delta'_{\bar{u}_{f_i},\bar{y}_{f_i}} - \delta_{\bar{u}_{f_i},\bar{y}_{f_i}}\| > \delta_{\bar{u}_{f_i},\bar{y}_{f_i}}\end{aligned} \tag{47}$$

where $Dev_{t_f\ldots t_d}(\tilde{x}^{\mathrm{T}}_{sub,\bar{u}_{f_i},\bar{y}_{f_i}}, \bar{u}_{f,i}, f_d x^{\mathrm{T}}_{sub,\bar{u}_{f_i},\bar{y}_{f_i}}, u_{f_i}) = \int_{t_f}^{t_{f+1}}(dev(\tilde{x}^{\mathrm{T}}_{sub,\bar{u}_{f_i},\bar{y}_{f_i}}, \bar{u}_{f,i}, f_d) - G_{sub,\bar{u}_{f_i},\bar{y}_{f_i}}([x^{\mathrm{T}}_{sub,\bar{u}_{f_i},\bar{y}_{f_i}}, \bar{x}^{\mathrm{T}}_{sub,\bar{u}_{f_i},\bar{y}_{f_i}}]^{\mathrm{T}})u_{f_i})d\tau + \cdots + \int_{t_{d-1}}^{t_d}(dev(\tilde{x}^{\mathrm{T}}_{sub,\bar{u}_{f_i},\bar{y}_{f_i}}, \bar{u}_{f,i}, f_d) - G_{sub,\bar{u}_{f_i},\bar{y}_{f_i}}([x^{\mathrm{T}}_{sub,\bar{u}_{f_i},\bar{y}_{f_i}}, \bar{x}^{\mathrm{T}}_{sub,\bar{u}_{f_i},\bar{y}_{f_i}}]^{\mathrm{T}})u_{f_i})d\tau$, $dev(\tilde{x}^{\mathrm{T}}_{sub,\bar{u}_{f_i},\bar{y}_{f_i}}, \tilde{x}^{\mathrm{T}}_{sub,u_{f_i},\bar{y}_{f_i}}, u_{sub,i}, f_d) = \tilde{f}_{sub,\bar{u}_{f_i},\bar{y}_{f_i}}([\tilde{x}^{\mathrm{T}}_{sub,\bar{u}_{f_i},\bar{y}_{f_i}}, \hat{\tilde{x}}^{\mathrm{T}}_{sub,\bar{u}_{f_i},\bar{y}_{f_i}}]^{\mathrm{T}}) + \tilde{G}_{sub,\bar{u}_{f_i},\bar{y}_{f_i}}([\tilde{x}^{\mathrm{T}}_{sub,\bar{u}_{f_i},\bar{y}_{f_i}}, \hat{\tilde{x}}^{\mathrm{T}}_{sub,\bar{u}_{f_i},\bar{y}_{f_i}}]^{\mathrm{T}})u_{sub,i} - \tilde{f}_{sub,\bar{u}_{f_i},\bar{y}_{f_i}}([\tilde{x}^{\mathrm{T}}_{sub,u_{f_i},y_{f_i}}, \hat{\tilde{x}}^{\mathrm{T}}_{sub,u_{f_i},y_{f_i}}]^{\mathrm{T}}) - \tilde{G}_{sub,\bar{u}_{f_i},\bar{y}_{f_i}}([\tilde{x}^{\mathrm{T}}_{sub,u_{f_i},y_{f_i}}, \hat{\tilde{x}}^{\mathrm{T}}_{sub,u_{f_i},y_{f_i}}]^{\mathrm{T}})u_{sub,i}$, where $u_{sub,i}$ is properly defined and f_d is the deviation of state estimates value from system states after fault occurrence:

$$\begin{aligned}f_d &= \hat{x}_{\bar{u}_{f_i},\bar{y}_{f_i}} - \hat{x}_{u_{f_i},y_{f_i}} = T'^{-1}(\hat{\zeta}, u_i) - T'^{-1}(\hat{\zeta}_{faultfree}, u_{f_i} + u_i) \\ &= T'^{-1}(\hat{\zeta}, u_i) - T'^{-1}(\hat{\zeta}, u_{f_i} + u_i) + T'^{-1}(\hat{\zeta}, u_{f_i} + u_i) - T'^{-1}(\hat{\zeta}_{faultfree}, u_{f_i} + u_i)\end{aligned} \tag{48}$$

Prepared using rncauth.cls DOI: 10.1002/rnc

where $\hat{\zeta} = \hat{\zeta}_{faultfree} + H\int_{t_f}^{t_{f+1}} e^{(A-HC)(t_{f+1}-\tau)}y_{f_i}d\tau + \dots$

$+ H\int_{t_{d-1}}^{t_d} e^{(A-HC)(t_d-\tau)}y_{f_i}d\tau$, $\vartheta(\frac{A_{0,sub,i,j}}{\varepsilon}, H_{sub,\bar{u}_{f_i},\bar{y}_{f_i}}, y_{f_i}) =$

$\int_{t_f}^{t_{f+1}} e^{\frac{A_{0,sub,\bar{u}_{f_i},\bar{y}_{f_i}}}{\varepsilon}(t_{f+1}-\tau)}[D_{sub,\bar{u}_{f_i},\bar{y}_{f_i}}]^{-1}H_{sub,\bar{u}_{f_i},\bar{y}_{f_i}}y_{f_i}d\tau + \dots$

$+ \int_{t_{d-1}}^{t_d} e^{\frac{A_{0,sub,\bar{u}_{f_i},\bar{y}_{f_i}}}{\varepsilon}(t_d-\tau)}[D_{sub,\bar{u}_{f_i},\bar{y}_{f_i}}]^{-1}H_{sub,\bar{u}_{f_i},\bar{y}_{f_i}}y_{f_i}d\tau,$

$f_{d,u_{f_i}} = T^{-1}(\zeta, u_{f_i}+u_i) - T^{-1}(\zeta, u_i)$ and $\delta'_{\bar{u}_{f_i},\bar{y}_{f_i}} = E'_{s,\bar{u}_{f_i},\bar{y}_{f_i}} = (\frac{1}{L'_{2,u_i}\beta_2(\varepsilon)} - L_{2,u_i}\beta_2(\varepsilon))E_{s,\bar{u}_{f_i},\bar{y}_{f_i}}$, then the fault is detected, i.e. $r_{\bar{u}_{f_i},\bar{y}_{f_i},d} > \delta_i$.

Proof

After fault occurrence (i.e., $t > t_f$), the prediction model corresponding to $r_{\bar{u}_{f_i},\bar{y}_{f_i}}$ takes the following form:

$$\dot{\hat{x}}_{sub,\bar{u}_{f_i},\bar{y}_{f_i}} = \tilde{f}_{sub,\bar{u}_{f_i},\bar{y}_{f_i}}([\tilde{x}^{\mathrm{T}}_{sub,u_{f_i},y_{f_i}}, \hat{\tilde{x}}^{\mathrm{T}}_{sub,u_{f_i},y_{f_i}}]^{\mathrm{T}}) + \tilde{G}_{sub,\bar{u}_{f_i},\bar{y}_{f_i}}([\tilde{x}^{\mathrm{T}}_{sub,u_{f_i},y_{f_i}}, \hat{\tilde{x}}^{\mathrm{T}}_{sub,u_{f_i},y_{f_i}}]^{\mathrm{T}})u_{sub,i} + dev(\tilde{x}^{\mathrm{T}}_{sub,\bar{u}_{f_i},\bar{y}_{f_i}}, \bar{u}_{f_i}, f_d) \tag{49}$$

where $u_{sub,i}$ is properly defined and $dev(\tilde{x}^{\mathrm{T}}_{sub,\bar{u}_{f_i},\bar{y}_{f_i}}, u_{sub,i}, f_d) = \tilde{f}_{sub,\bar{u}_{f_i},\bar{y}_{f_i}}([\tilde{x}^{\mathrm{T}}_{sub,\bar{u}_{f_i},\bar{y}_{f_i}}, \hat{\tilde{x}}^{\mathrm{T}}_{sub,\bar{u}_{f_i},\bar{y}_{f_i}}]^{\mathrm{T}}) + \tilde{G}_{sub,\bar{u}_{f_i},\bar{y}_{f_i}}([\tilde{x}^{\mathrm{T}}_{sub,\bar{u}_{f_i},\bar{y}_{f_i}}, \hat{\tilde{x}}^{\mathrm{T}}_{sub,\bar{u}_{f_i},\bar{y}_{f_i}}]^{\mathrm{T}})u_{sub,i} - \tilde{f}_{sub,\bar{u}_{f_i},\bar{y}_{f_i}}([\tilde{x}^{\mathrm{T}}_{sub,u_{f_i},y_{f_i}}, \hat{\tilde{x}}^{\mathrm{T}}_{sub,u_{f_i},y_{f_i}}]^{\mathrm{T}}) - \tilde{G}_{sub,\bar{u}_{f_i},\bar{y}_{f_i}}([\tilde{x}^{\mathrm{T}}_{sub,u_{f_i},y_{f_i}}, \hat{\tilde{x}}^{\mathrm{T}}_{sub,u_{f_i},y_{f_i}}]^{\mathrm{T}})u_{sub,i}$ and f_d is the deviation of state estimates from system states, after fault occurrence. To calculate f_d, we consider the corresponding observer to $r_{\bar{u}_{f_i},\bar{y}_{f_i}}$, and focus on the residual that breaches the threshold due to the occurrence of both the sensor and actuator fault (note that the analysis for residuals that are breached due to say, only the actuator or only the sensor faults are special cases of the below analysis). We then have:

$$\begin{aligned} \dot{\hat{\zeta}} &= A\hat{\zeta} + B\phi_0 + H(C\zeta + y_{f_i} - C\hat{\zeta}) \\ \hat{\zeta}(t_k) &= T'(\hat{x}(t_k), u_i(t_k)) \end{aligned} \tag{50}$$

By integration from t_f to t_d, we get:

$$\begin{aligned} \hat{\zeta} &= \hat{\zeta}(t_f) + \int_{t_f}^{t_{f+1}} e^{(A-HC)(t_{f+1}-\tau)}(B\phi_0 + HC\zeta)d\tau + \cdots + \int_{t_{d-1}}^{t_d} e^{(A-HC)(t_d-\tau)}(B\phi_0 + HC\zeta)d\tau \\ &+ H\int_{t_f}^{t_{f+1}} e^{(A-HC)(t_{f+1}-\tau)}y_{f_i}d\tau + \cdots + H\int_{t_{d-1}}^{t_d} e^{(A-HC)(t_d-\tau)}y_{f_i}d\tau \\ &= \hat{\zeta}_{faultfree} + H\int_{t_f}^{t_{f+1}} e^{(A-HC)(t_{f+1}-\tau)}y_{f_i}d\tau + \cdots + H\int_{t_{d-1}}^{t_d} e^{(A-HC)(t_d-\tau)}y_{f_i}d\tau \end{aligned} \tag{51}$$

Prepared using rncauth.cls DOI: 10.1002/rnc

where $\hat{\zeta}_{faultfree} = \hat{\zeta}(t_f) + \int_{t_f}^{t_{f+1}} e^{(A-HC)(t_{f+1}-\tau)}(B\phi_0 + HC\zeta)d\tau + \ldots$

$+ \int_{t_{d-1}}^{t_d} e^{(A-HC)(t_d-\tau)}(B\phi_0 + HC\zeta)d\tau$. Therefore, f_d is formulated as below:

$$\begin{aligned} f_d &= \hat{x}_{\bar{u}_{f_i},\bar{y}_{f_i}} - \hat{x}_{u_{f_i},y_{f_i}} = T'^{-1}(\hat{\zeta}, u_i) - T'^{-1}(\hat{\zeta}_{faultfree}, u_{f_i} + u_i) \\ &= T'^{-1}(\hat{\zeta}, u_i) - T'^{-1}(\hat{\zeta}, u_{f_i} + u_i) + T'^{-1}(\hat{\zeta}, u_{f_i} + u_i) - T'^{-1}(\hat{\zeta}_{faultfree}, u_{f_i} + u_i) \end{aligned} \tag{52}$$

Substituting f_d into Eq. 30 gives:

$$\begin{aligned} \dot{\tilde{e}}_{i,k} = \tilde{f}_{sub,\bar{u}_{f_i},\bar{y}_{f_i}} - f_{sub,\bar{u}_{f_i},\bar{y}_{f_i}}([x^{\mathrm{T}}_{sub,\bar{u}_{f_i},\bar{y}_{f_i}}, \bar{x}^{\mathrm{T}}_{sub,\bar{u}_{f_i},\bar{y}_{f_i}}]^{\mathrm{T}}) + (\tilde{G}_{sub,\bar{u}_{f_i},\bar{y}_{f_i}} \\ - G_{sub,\bar{u}_{f_i},\bar{y}_{f_i}}([x^{\mathrm{T}}_{sub,\bar{u}_{f_i},\bar{y}_{f_i}}, \bar{x}^{\mathrm{T}}_{sub,\bar{u}_{f_i},\bar{y}_{f_i}}]^{\mathrm{T}})u_{sub,i} + dev(\tilde{x}^{\mathrm{T}}_{sub,\bar{u}_{f_i},\bar{y}_{f_i}}, \bar{u}_{f,i}, f_d) \\ - G_{sub,\bar{u}_{f_i},\bar{y}_{f_i}}([x^{\mathrm{T}}_{sub,\bar{u}_{f_i},\bar{y}_{f_i}}, \bar{x}^{\mathrm{T}}_{sub,\bar{u}_{f_i},\bar{y}_{f_i}}]^{\mathrm{T}})u_{f_i} \end{aligned} \tag{53}$$

By integration from t_f to t_d, we obtain:

$$\begin{aligned} \tilde{e}_{i,t_d} = \tilde{e}_{i,t_f} + \int_{t_f}^{t_{f+1}} (\tilde{f}_{sub,\bar{u}_{f_i},\bar{y}_{f_i}} - f_{sub,i}([x^{\mathrm{T}}_{sub,i}, \bar{x}^{\mathrm{T}}_{sub,i}]^{\mathrm{T}}) + (\tilde{G}_{sub,\bar{u}_{f_i},\bar{y}_{f_i}} \\ - G_{sub,\bar{u}_{f_i},\bar{y}_{f_i}}([x^{\mathrm{T}}_{sub,\bar{u}_{f_i},\bar{y}_{f_i}}, \bar{x}^{\mathrm{T}}_{sub,\bar{u}_{f_i},\bar{y}_{f_i}}]^{\mathrm{T}}))u_{prescribed,i})d\tau + \ldots \\ + \int_{t_{d-1}}^{t_d} (\tilde{f}_{sub,\bar{u}_{f_i},\bar{y}_{f_i}} - f_{sub,\bar{u}_{f_i},\bar{y}_{f_i}}([x^{\mathrm{T}}_{sub,\bar{u}_{f_i},\bar{y}_{f_i}}, \bar{x}^{\mathrm{T}}_{sub,\bar{u}_{f_i},\bar{y}_{f_i}}]^{\mathrm{T}}) + \\ \int_{t_{d-1}}^{t_d} (\tilde{G}_{sub,\bar{u}_{f_i},\bar{y}_{f_i}} - G_{sub,\bar{u}_{f_i},\bar{y}_{f_i}}([x^{\mathrm{T}}_{sub,\bar{u}_{f_i},\bar{y}_{f_i}}, \bar{x}^{\mathrm{T}}_{sub,\bar{u}_{f_i},\bar{y}_{f_i}}]^{\mathrm{T}}))u_{prescribed,i})d\tau + \\ \int_{t_f}^{t_{f+1}} (dev(\tilde{x}^{\mathrm{T}}_{sub,\bar{u}_{f_i},\bar{y}_{f_i}}, \bar{u}_{f,i,sub}, f_d) - G_{sub,\bar{u}_{f_i},\bar{y}_{f_i}}([x^{\mathrm{T}}_{sub,\bar{u}_{f_i},\bar{y}_{f_i}}, \bar{x}^{\mathrm{T}}_{sub,\bar{u}_{f_i},\bar{y}_{f_i}}]^{\mathrm{T}})u_{f_i})d\tau \\ + \cdots + \int_{t_{d-1}}^{t_d} (dev(\tilde{x}^{\mathrm{T}}_{sub,\bar{u}_{f_i},\bar{y}_{f_i}}, \bar{u}_{f,i,sub}, f_d) - G_{sub,\bar{u}_{f_i},\bar{y}_{f_i}}([x^{\mathrm{T}}_{sub,\bar{u}_{f_i},\bar{y}_{f_i}}, \bar{x}^{\mathrm{T}}_{sub,\bar{u}_{f_i},\bar{y}_{f_i}}]^{\mathrm{T}})u_{f_i})d\tau \\ = \tilde{e}_{i,faultfree} + Dev_{t_f \ldots t_d}(\tilde{x}^{\mathrm{T}}_{sub,\bar{u}_{f_i},\bar{y}_{f_i}}, \bar{u}_{f,i,sub}, f_d, x^{\mathrm{T}}_{sub,\bar{u}_{f_i},\bar{y}_{f_i}}, u_{f_i}) \end{aligned} \tag{54}$$

where $\tilde{e}_{i,faultfree} = \tilde{e}_{i,t_f} + \int_{t_f}^{t_{f+1}} (\tilde{f}_{sub,\bar{u}_{f_i},\bar{y}_{f_i}} - f_{sub,\bar{u}_{f_i},\bar{y}_{f_i}}([x^{\mathrm{T}}_{sub,\bar{u}_{f_i},\bar{y}_{f_i}}, \bar{x}^{\mathrm{T}}_{sub,\bar{u}_{f_i},\bar{y}_{f_i}}]^{\mathrm{T}}) +$

$(\tilde{G}_{sub,\bar{u}_{f_i},\bar{y}_{f_i}} - G_{sub,\bar{u}_{f_i},\bar{y}_{f_i}}([x^{\mathrm{T}}_{sub,\bar{u}_{f_i},\bar{y}_{f_i}}, \bar{x}^{\mathrm{T}}_{sub,\bar{u}_{f_i},\bar{y}_{f_i}}]^{\mathrm{T}}))u_{prescribed,i})d\tau + \ldots$

$+ \int_{t_{d-1}}^{t_d} (\tilde{f}_{sub,\bar{u}_{f_i},\bar{y}_{f_i}} - f_{sub,\bar{u}_{f_i},\bar{y}_{f_i}}([x^{\mathrm{T}}_{sub,\bar{u}_{f_i},\bar{y}_{f_i}}, \bar{x}^{\mathrm{T}}_{sub,\bar{u}_{f_i},\bar{y}_{f_i}}]^{\mathrm{T}})$

$+ (\tilde{G}_{sub,\bar{u}_{f_i},\bar{y}_{f_i}} - G_{sub,\bar{u}_{f_i},\bar{y}_{f_i}}([x^{\mathrm{T}}_{sub,\bar{u}_{f_i},\bar{y}_{f_i}}, \bar{x}^{\mathrm{T}}_{sub,\bar{u}_{f_i},\bar{y}_{f_i}}]^{\mathrm{T}}), u_{prescribed,i})d\tau,$

$Dev_{t_f \ldots t_d}(\tilde{x}^{\mathrm{T}}_{sub,\bar{u}_{f_i},\bar{y}_{f_i}}, \bar{u}_{f,i,sub}, f_d, x^{\mathrm{T}}_{sub,\bar{u}_{f_i},\bar{y}_{f_i}}, u_{f_i}) = \int_{t_f}^{t_{f+1}} (dev(\tilde{x}^{\mathrm{T}}_{sub,\bar{u}_{f_i},\bar{y}_{f_i}}, \bar{u}_{f,i,sub}, f_d)$

$-G_{sub,\bar{u}_{f_i},\bar{y}_{f_i}}([x^{\mathrm{T}}_{sub,\bar{u}_{f_i},\bar{y}_{f_i}}, \bar{x}^{\mathrm{T}}_{sub,\bar{u}_{f_i},\bar{y}_{f_i}}]^{\mathrm{T}})u_{f_i})d\tau + \cdots + \int_{t_{d-1}}^{t_d} (dev(\tilde{x}^{\mathrm{T}}_{sub,\bar{u}_{f_i},\bar{y}_{f_i}}, \bar{u}_{f,i,sub}, f_d)$

$-G_{sub,\bar{u}_{f_i},\bar{y}_{f_i}}([x^{\mathrm{T}}_{sub,\bar{u}_{f_i},\bar{y}_{f_i}}, \bar{x}^{\mathrm{T}}_{sub,\bar{u}_{f_i},\bar{y}_{f_i}}]^{\mathrm{T}})u_{f_i})d\tau.$

Prepared using rncauth.cls DOI: 10.1002/rnc

Now by applying the triangular inequality, we get:

$$\begin{aligned}\|\tilde{x}_{sub,}(t_d) - x_{sub,i}(t_d)\| &= \|\tilde{e}_{i,k}(t_d)\| \\ &\geq \|Dev_{t_f \ldots t_d}(\tilde{x}^{\mathrm{T}}_{sub,\bar{u}_{f_i},\bar{y}_{f_i}}, \bar{u}_{f,i,sub}, f_d, x^{\mathrm{T}}_{sub,\bar{u}_{f_i},\bar{y}_{f_i}}, u_{f_i})\| \\ &- E_p^{\bar{u}_{f_i},\bar{y}_{f_i}}\end{aligned} \tag{55}$$

After fault occurrence the Eq. 33 takes the following form:

$$\begin{aligned}\dot{e}_{sub,i,j} = \frac{1}{\varepsilon} A_{0,sub,\bar{u}_{f_i},\bar{y}_{f_i}} e_{sub,\bar{u}_{f_i},\bar{y}_{f_i}} + B_{sub,\bar{u}_{f_i},\bar{y}_{f_i}}(\phi_{sub,\bar{u}_{f_i},\bar{y}_{f_i}} - \phi_{0,sub,\bar{u}_{f_i},\bar{y}_{f_i}}) \\ + \eta_{i,sub,\bar{u}_{f_i},\bar{y}_{f_i}} + [D_{sub,\bar{u}_{f_i},\bar{y}_{f_i}}]^{-1} H_{sub,\bar{u}_{f_i},\bar{y}_{f_i}} y_{f_i}\end{aligned} \tag{56}$$

By integration from t_f to t_d, we obtain:

$$\begin{aligned}e_{sub,\bar{u}_{f_i},\bar{y}_{f_i}}(t_d) = e_{sub,i,j}(t_f) + \int_{t_f}^{t_{f+1}} e^{\frac{A_{0,sub,\bar{u}_{f_i},\bar{y}_{f_i}}}{\varepsilon}(t_{f+1}-\tau)}(B_{sub,i,j}(\phi_{sub,\bar{u}_{f_i},\bar{y}_{f_i}} - \phi_{0,sub,\bar{u}_{f_i},\bar{y}_{f_i}}) \\ + \eta_{i,sub,\bar{u}_{f_i},\bar{y}_{f_i}})d\tau + \cdots + \int_{t_{d-1}}^{t_d} e^{\frac{A_{0,sub,i,j}}{\varepsilon}(t_d-\tau)}(B_{sub,i,j}(\phi_{sub,\bar{u}_{f_i},\bar{y}_{f_i}} - \phi_{0,sub,\bar{u}_{f_i},\bar{y}_{f_i}}) \\ + \eta_{i,sub,\bar{u}_{f_i},\bar{y}_{f_i}})d\tau + \int_{t_f}^{t_{f+1}} e^{\frac{A_{0,sub,\bar{u}_{f_i},\bar{y}_{f_i}}}{\varepsilon}(t_{f+1}-\tau)}[D_{sub,\bar{u}_{f_i},\bar{y}_{f_i}}]^{-1} H_{sub,\bar{u}_{f_i},\bar{y}_{f_i}} y_{f_i} d\tau \\ + \cdots + \int_{t_{d-1}}^{t_d} e^{\frac{A_{0,sub,\bar{u}_{f_i},\bar{y}_{f_i}}}{\varepsilon}(t_d-\tau)}[D_{sub,\bar{u}_{f_i},\bar{y}_{f_i}}]^{-1} H_{sub,\bar{u}_{f_i},\bar{y}_{f_i}} y_{f_i} d\tau \\ = e_{i,faultfree} + \vartheta(\frac{A_{0,sub,\bar{u}_{f_i},\bar{y}_{f_i}}}{\varepsilon}, H_{sub,\bar{u}_{f_i},\bar{y}_{f_i}}, y_{f_i})\end{aligned} \tag{57}$$

where $e_{i,faultfree} = e_{sub,\bar{u}_{f_i},\bar{y}_{f_i}}(t_f) + \int_{t_f}^{t_{f+1}} e^{\frac{A_{0,sub,\bar{u}_{f_i},\bar{y}_{f_i}}}{\varepsilon}(t_{f+1}-\tau)}(B_{sub,\bar{u}_{f_i},\bar{y}_{f_i}}(\phi_{sub,\bar{u}_{f_i},\bar{y}_{f_i}} - \phi_{0,sub,i,j}) + \eta_{i,sub,\bar{u}_{f_i},\bar{y}_{f_i}})d\tau + \cdots + \int_{t_{d-1}}^{t_d} e^{\frac{A_{0,sub,\bar{u}_{f_i},\bar{y}_{f_i}}}{\varepsilon}(t_d-\tau)}(B_{sub,\bar{u}_{f_i},\bar{y}_{f_i}}(\phi_{sub,\bar{u}_{f_i},\bar{y}_{f_i}} - \phi_{0,sub,\bar{u}_{f_i},\bar{y}_{f_i}}) + \eta_{i,sub,\bar{u}_{f_i},\bar{y}_{f_i}})d\tau$,
$\vartheta(\frac{A_{0,sub,\bar{u}_{f_i},\bar{y}_{f_i}}}{\varepsilon}, H_{sub,\bar{u}_{f_i},\bar{y}_{f_i}}, y_{f_i}) = \int_{t_f}^{t_{f+1}} e^{\frac{A_{0,sub,\bar{u}_{f_i},\bar{y}_{f_i}}}{\varepsilon}(t_{f+1}-\tau)}[D_{sub,\bar{u}_{f_i},\bar{y}_{f_i}}]^{-1} H_{sub,\bar{u}_{f_i},\bar{y}_{f_i}} y_{f_i} d\tau + \cdots + \int_{t_{d-1}}^{t_d} e^{\frac{A_{0,sub,\bar{u}_{f_i},\bar{y}_{f_i}}}{\varepsilon}(t_d-\tau)}[D_{sub,\bar{u}_{f_i},\bar{y}_{f_i}}]^{-1} H_{sub,\bar{u}_{f_i},\bar{y}_{f_i}} y_{f_i} d\tau$. By applying the triangular inequality, we get:

$$\|e(t_{k+1})\| \geq E_{s,\bar{u}_{f_i},\bar{y}_{f_i}} - \|\vartheta(\frac{A_{0,sub,\bar{u}_{f_i},\bar{y}_{f_i}}}{\varepsilon}, H_{sub,\bar{u}_{f_i},\bar{y}_{f_i}}, y_{f_i})\| \tag{58}$$

For the residual that breaches the threshold due to both sensor and actuator fault, we have:

$$\begin{aligned}x_{sub,\bar{u}_{f_i},\bar{y}_{f_i}}(t_d) - \hat{x}_{sub,\bar{u}_{f_i},\bar{y}_{f_i}}(t_d) = T^{-1}(\zeta, u_{f_i} + u_i) - T'^{-1}(\hat{\zeta}, u_i) = T^{-1}(\zeta, u_{f_i} + u_i) \\ - T^{-1}(\zeta, u_i) + T^{-1}(\zeta, u_i) - T'^{-1}(\hat{\zeta}, u_i)\end{aligned} \tag{59}$$

Prepared using rncauth.cls
DOI: 10.1002/rnc

By using Lipschitz property of T'^{-1} and Eq. 19, after applying the triangular inequality, we get:

$$\|x_{sub,\bar{u}_{f_i},\bar{y}_{f_i}}(t_d) - \hat{x}_{sub,\bar{u}_{f_i},\bar{y}_{f_i}}(t_d)\| \geq L_{2,u_i}\beta_2(\varepsilon)E_{s,\bar{u}_{f_i},\bar{y}_{f_i}} + \bar{\theta}_{sub,l}\Delta + E'_{s,\bar{u}_{f_i},\bar{y}_{f_i}} + \|f_{d,u_{f_i}}\| - \frac{1}{L'_{2,u_i}\beta_2(\varepsilon)}\|\vartheta(\frac{A_{0,sub,\bar{u}_{f_i},\bar{y}_{f_i}}}{\varepsilon}, H_{sub,\bar{u}_{f_i},\bar{y}_{f_i}}, y_{f_i})\| \tag{60}$$

where $E'_{s,\bar{u}_{f_i},\bar{y}_{f_i}} = (\frac{1}{L'_{2,u_i}\beta_2(\varepsilon)} - L_{2,u_i}\beta_2(\varepsilon))E_{s,\bar{u}_{f_i},\bar{y}_{f_i}}$ and $f_{d,u_{f_i}} = T^{-1}(\zeta, u_{f_i} + u_i) - T^{-1}(\zeta, u_i)$. Therefore by using Eqs. 55, 60 and triangular inequality, we obtain:

$$r_{i,d} = \|\tilde{x}_{sub,\bar{u}_{f_i},\bar{y}_{f_i}}(t_d) - \hat{x}_{sub,\bar{u}_{f_i},\bar{y}_{f_i}}(t_d)\| \geq \|\frac{1}{L'_{2,u_i}\beta_2(\varepsilon)}\|\vartheta(\frac{A_{0,sub,\bar{u}_{f_i},\bar{y}_{f_i}}}{\varepsilon}, H_{sub,\bar{u}_{f_i},\bar{y}_{f_i}}, y_{f_i})\| + \|f_{d,u_{f_i}}\| + \|Dev_{t_f\ldots t_d}(\tilde{x}^{\mathrm{T}}_{sub,\bar{u}_{f_i},\bar{y}_{f_i}}, \bar{u}_{f_i}, f_d, x^{\mathrm{T}}_{sub,\bar{u}_{f_i},\bar{y}_{f_i}}, u_{f_i})\| - \delta_{\bar{u}_{f_i},\bar{y}_{f_i}} - \delta'_{\bar{u}_{f_i},\bar{y}_{f_i}}\| \tag{61}$$

where $\delta'_{\bar{u}_{f_i},\bar{y}_{f_i}} = E'_{s,\bar{u}_{f_i},\bar{y}_{f_i}}$. Therefore it follows that if Eq. 47 holds, $t_f \geq t_{k'}$, $r_{\bar{u}_{f_i},\bar{y}_{f_i},d} > \delta_{i,\bar{u}_{f_i},\bar{y}_{f_i}}$. □

4.1. Isolability Condition

Having presented the detectability condition corresponding to different faulty scenarios, Theorem 3 presents the fault isolation logic for the identification of faulty component that also holds as isolability condition corresponding to fault $\theta_{f,j}$. The proof of Theorem 3 follows a similar line of Theorem 1 presented [6], and hence is omitted here.

Theorem 3. Consider the system of Eq. 1, for which Assumptions 1-5 hold. If $t \geq t_d$ and $r_{i,t_d} > \delta_i$ for all $i \in \{1, \ldots, n_f\}\backslash j$, then $\Theta_{f,j}(t) \neq 0$ for some $t \in [t_d, t_{d+1})$.

Remark 6. Theorem 3 states that a fault is isolated when the corresponding sensitive residuals breach their threshold, forming a unique breaching pattern or fault signature. Note that in the proposed framework, there exists a unique signature (in terms of residuals breaching pattern) corresponding to each fault scenario that enables distinguishing between different fault scenarios and leads to fault isolation (see e.g., [6] for further details regarding expected breaching patterns corresponding to single or multiple fault scenarios). The key when dealing with uncertainty, however, is to ensure that such unique fault signatures continue to exist in the presence of

Prepared using rncauth.cls DOI: 10.1002/rnc

uncertainty, which is achieved by appropriate choice of the thresholds that are cognizant of the presence of uncertainty.

Remark 7. Note that the proposed approach does not make any assumptions on the nature of the controller. In particular, even if the controller is able to reject the effect of the fault, the FDI mechanism enables fault detection and isolation subject to the corresponding detectability conditions being satisfied.

Remark 8. The proposed approach provides the specific observer and FDI design, and backs it up with a rigorous analysis that establishes error bounds and thresholds based on the system characteristics. Note however that the calculation of various quantities (utilized in the proving the results) is not required for the actual implementation of the proposed approach. In practice, the rigorous analysis can be utilized to provide confidence in the FDI capabilities of the proposed filters and to guide the selection of the parameters (as is done in the simulation results).

5. SIMULATION EXAMPLE

In this section, we consider a continuous-stirred tank reactor (CSTR) example. The feed to the reactor includes A and B at a flow rate F, concentrations C_{A0} and C_{B0}, and temperature T_0. In the reactor, three reversible elementary exothermic reactions take place adiabatically as follows:

$$\begin{aligned} \mathrm{A} + \mathrm{B} &\underset{k_{-1\mathrm{A}}}{\overset{k_{1\mathrm{A}}}{\rightleftharpoons}} \mathrm{C} \\ \mathrm{A} + \mathrm{C} &\underset{k_{-2\mathrm{A}}}{\overset{k_{2\mathrm{A}}}{\rightleftharpoons}} \mathrm{D} \\ \mathrm{C} + \mathrm{D} &\underset{k_{-3\mathrm{C}}}{\overset{k_{3\mathrm{C}}}{\rightleftharpoons}} \mathrm{U} \end{aligned} \tag{62}$$

where C is the intermediate product, D is the desired product, U is the undesired product, and $k_{1\mathrm{A}}$, $k_{-1\mathrm{A}}$, $k_{2\mathrm{A}}$, $k_{-2\mathrm{A}}$, $k_{3\mathrm{C}}$, and $k_{-3\mathrm{C}}$ are specific rates of reaction for the forward and reverse reactions,

Prepared using rncauth.cls
DOI: 10.1002/rnc

respectively. The mathematical model of this chemical reactor is as follows:

$$\begin{aligned}
\dot{C}_{\mathrm{A}} &= \frac{F}{V}(C_{\mathrm{A0}} - C_{\mathrm{A}}) + r_{\mathrm{1A,\,forward}} + r_{\mathrm{1A,\,reverse}} + r_{\mathrm{2A,\,forward}} + r_{\mathrm{2A,\,reverse}} \\
\dot{C}_{\mathrm{B}} &= \frac{F}{V}(C_{\mathrm{B0}} - C_{\mathrm{B}}) + r_{\mathrm{1A,\,forward}} + r_{\mathrm{1A,\,reverse}} \\
\dot{C}_{\mathrm{C}} &= -\frac{F}{V}C_{\mathrm{C}} - r_{\mathrm{1A,\,forward}} - r_{\mathrm{1A,\,reverse}} + r_{\mathrm{2A,\,forward}} + r_{\mathrm{2A,\,reverse}} + r_{\mathrm{3C,\,forward}} + r_{\mathrm{3C,\,reverse}} \\
\dot{C}_{\mathrm{U}} &= -\frac{F}{V}C_{\mathrm{U}} - r_{\mathrm{3C,\,forward}} - r_{\mathrm{3C,\,reverse}} \\
\dot{C}_{\mathrm{D}} &= -\frac{F}{V}C_{\mathrm{D}} - r_{\mathrm{2A,\,forward}} - r_{\mathrm{2A,\,reverse}} + r_{\mathrm{3C,\,forward}} + r_{\mathrm{3C,\,reverse}} \\
\dot{T}_{\mathrm{R}} &= \frac{F}{V}(T_0 - T_{\mathrm{R}}) + \frac{(-\Delta H_1)}{\rho c_p}(r_{\mathrm{1A,\,forward}} + r_{\mathrm{1A,\,reverse}}) + \frac{(-\Delta H_2)}{\rho c_p}(r_{\mathrm{2A,\,forward}} \\
&\quad + r_{\mathrm{2A,\,reverse}}) + \frac{(-\Delta H_3)}{\rho c_p}(r_{\mathrm{3C,\,forward}} + r_{\mathrm{3C,\,reverse}})
\end{aligned} \tag{63}$$

where C_i is the concentration of species i, $i = $ A, B, C, U, D, T_{R} is the temperature in the reactor, V is the volume of the reactor, ΔH_i, $i =$1, 2, 3 are the enthalpy of the ith reaction, and ρ and c_p are the density and the heat capacity of the fluid in the reactor, respectively. The reaction rates are as follows:

$$\begin{aligned}
r_{\mathrm{1A,\,forward}} &= -k_{\mathrm{1A0}}e^{-E_1/(RT_{\mathrm{R}})}C_{\mathrm{A}}C_{\mathrm{B}} \\
r_{\mathrm{1A,\,reverse}} &= k_{\mathrm{-1A0}}e^{-E_{-1}/(RT_{\mathrm{R}})}C_{\mathrm{C}} \\
r_{\mathrm{2A,\,forward}} &= -k_{\mathrm{2A0}}e^{-E_2/(RT_{\mathrm{R}})}C_{\mathrm{A}}C_{\mathrm{C}} \\
r_{\mathrm{2A,\,reverse}} &= k_{\mathrm{-2A0}}e^{-E_{-2}/(RT_{\mathrm{R}})}C_{\mathrm{D}} \\
r_{\mathrm{3C,\,forward}} &= -k_{\mathrm{3C0}}e^{-E_3/(RT_{\mathrm{R}})}C_{\mathrm{C}}C_{\mathrm{D}} \\
r_{\mathrm{3C,\,reverse}} &= k_{\mathrm{-3C0}}e^{-E_{-3}/(RT_{\mathrm{R}})}C_{\mathrm{U}}
\end{aligned} \tag{64}$$

where k_{ij0} and k_{-ij0}, $i =$1, 2, 3, $j =$A, C are the pre-exponential constants for the forward and reverse reactions, respectively, E_i and E_{-i}, $i =$1, 2, 3 are the activation energies for the forward and reverse reactions, respective, and R is the ideal gas constant. The process parameters can be found in Table I. The control objective under normal conditions is to operate the process at the nominal operating point, where $C_{\mathrm{A}} = 0.828$ kmol/m^3, $C_{\mathrm{B}} = 0.743$ kmol/m^3, $C_{\mathrm{C}} = 0.976$ kmol/m^3, $C_{\mathrm{U}} = 0.365$ kmol/m^3, $C_{\mathrm{D}} = 0.550$ kmol/m^3, and $T_{\mathrm{R}} = 425.4$ K. The manipulated input variables ae $u = [C_{\mathrm{A0}}, T_0]^{\mathrm{T}}$, where $0 \leq C_{\mathrm{A0}} \leq 10$ kmol/m^3 and $300 \leq T_0 \leq 350$ K, and the measured outputs are $y = [C_{\mathrm{A}}, C_{\mathrm{B}}, C_{\mathrm{C}}, C_{\mathrm{D}}, T_{\mathrm{R}}]^{\mathrm{T}}$(see [6] for details about control and observer design).

Prepared using rncauth.cls
DOI: 10.1002/rnc

Table I. Process parameters for the chemical reactor example of Section 4.

Parameter	Value	Unit
F	0.12	m^3/min
V	1	m^3
k_{1A0}	1.50×10^{10}	min^{-1}
k_{-1A0}	1.25×10^{10}	min^{-1}
k_{2A0}	1.50×10^{10}	min^{-1}
k_{-2A0}	1.25×10^{10}	min^{-1}
k_{3C0}	1.50×10^{10}	min^{-1}
k_{-3C0}	1.25×10^{10}	min^{-1}
E_1	6.5×10^4	kJ/kmol
E_{-1}	6.6×10^4	kJ/kmol
E_2	6.8×10^4	kJ/kmol
E_{-2}	6.6×10^4	kJ/kmol
E_3	6.8×10^4	kJ/kmol
E_{-3}	6.6×10^4	kJ/kmol
R	8.314	kJ/kmol·K
$-\Delta H_1$	1.50×10^4	kJ/kmol
$-\Delta H_2$	0.75×10^4	kJ/kmol
$-\Delta H_3$	0.70×10^4	kJ/kmol
ρ	1000	kg/m^3
c_p	0.315	kJ/kg·K
C_{A0}	3	kmol/m^3
C_{B0}	4	kmol/m^3
T_0	320	K

The system of Eq. (63) is subject to modeling uncertainty and measurement noise. In particular, the actual values of k_{1A0} and k_{2A0} are 10% less than their nominal values. Furthermore, the flow rate fluctuates with time, with the actual flow rate being $1 + 0.05\sin(t)$ times of its nominal value. The known bounds on each uncertainty is 15%, 15% and 5% of the absolute nominal values.

Prepared using rncauth.cls
DOI: 10.1002/rnc

Table II. Faults to which the residuals are insensitive and thresholds for the fault isolation design of the example in Section 5 based on the proposed framework in 4.

Residual	Faults	Threshold	Residual	Faults	Threshold
r_1	y_{f_1}	0.1	r_2	y_{f_2}	0.1
r_3	y_{f_3}	0.1	r_4	y_{f_4}	0.1
r_5	y_{f_5}	0.5	r_6	y_{f_1}, y_{f_2}	0.1
r_7	y_{f_1}, y_{f_3}	0.1	r_8	y_{f_1}, y_{f_4}	0.1
r_9	y_{f_1}, y_{f_5}	0.5	r_{10}	y_{f_2}, y_{f_3}	0.1
r_{11}	y_{f_2}, y_{f_4}	0.1	r_{12}	y_{f_2}, y_{f_5}	0.33
r_{13}	y_{f_3}, y_{f_4}	0.1	r_{14}	y_{f_3}, y_{f_5}	2.8
r_{15}	y_{f_4}, y_{f_5}	1.7	r_{16}	u_{f_2}	0.002
r_{17}	u_{f_2}, y_{f_5}	0.002	r_{18}	u_{f_1}	0.1
r_{19}	u_{f_1}, y_{f_1}	0.3	r_{20}	u_{f_1}, u_{f_2}	0.002
r_{21}	u_{f_1}, y_{f_2}	0.12	r_{22}	u_{f_1}, y_{f_3}	0.13
r_{23}	u_{f_1}, y_{f_4}	0.14	r_{24}	u_{f_1}, y_{f_5}	0.5
r_{25}	u_{f_2}, y_{f_1}	0.002	r_{26}	u_{f_2}, y_{f_2}	0.002
r_{27}	u_{f_2}, y_{f_3}	0.003	r_{28}	u_{f_2}, y_{f_4}	0.004

The concentration and temperature measurements have combinations of 5 Hz sinusoidal noises. The magnitudes over each 0.5 min follow a normal distribution with the standard deviations being 0.02 kmol/m^3 and 0.5 K for concentrations and temperatures, respectively. The noisy measurements are passed through a first-order low-pass filter with the filter time constant being 3 seconds. The thresholds are selected based on Eq. 28 via simulations. To this end, a value slightly larger than the summation of the maximum observed values for $\|\tilde{x}_{sub,i,j}(t_{k+1}) - x_{sub,i,j}(t_{k+1})\|$

Prepared using rncauth.cls
DOI: 10.1002/rnc

and $\|x_{sub,i,j}(t_{k+1}) - \hat{x}_{sub,i,j}(t_{k+1})\|$, by considering all possible combinations of the bounds on uncertainties is selected as the corresponding threshold for each residual, as shown in Table II.

Remark 9. Note that in the case of systems with relatively low degree of nonlinearity like single link robot arm of [14], the parameters in Eq. 27 can be specified and as a result, the Eq. 27 can be used directly for defining thresholds. However, when it comes to highly nonlinear systems like the CSTR example used here, it is not possible to find all of the constants in the Eq. 27. Instead we used simulations to determine the suprema of $\|\tilde{x}_{sub,i,j}(t_{k+1}) - x_{sub,i,j}(t_{k+1})\|$ and $\|x_{sub,i,j}(t_{k+1}) - \hat{x}_{sub,i,j}(t_{k+1})\|$, to in turn utilize as the threshold values suggested by Eq. 28. Note that the main purpose of deriving a mathematical formula for thresholds (Eq. 39) in this work is to establish the ability of the proposed scheme to achieve fault detection and isolation in the presence of uncertainty rigorously.

Table III. Detectability constants ($\bar{\delta}$) for each residual for a case where abrupt fault of $u_{f_2} = 0.1$ in u_2 takes place at time $t_f = 7.5$ min

Residual	$\bar{\delta}$	Threshold	Residual	$\bar{\delta}$	Threshold
r_1	0.047	0.1	r_2	0.056	0.1
r_3	0.052	0.1	r_4	0.048	0.1
r_5	0.22	0.5	r_6	0.051	0.1
r_7	0.051	0.1	r_8	0.051	0.1
r_9	0.18	0.48	r_{10}	0.05	0.1
r_{11}	0.05	0.1	r_{12}	0.33	0.4
r_{13}	0.05	0.1	r_{14}	0.824	1.7
r_{15}	0.555	2.8	r_{16}	0	0.002
r_{17}	0	0.003	r_{18}	0.059	0.1
r_{19}	0.059	0.3	r_{20}	0	0.001
r_{21}	0.0745	0.12	r_{22}	0.066	0.13
r_{23}	0.06	0.14	r_{24}	0.22	0.5
r_{25}	0	0.002	r_{26}	0	0.002
r_{27}	0	0.003	r_{28}	0	0.004

Prepared using rncauth.cls
DOI: 10.1002/rnc

We first show the application of the detectability condition presented in Theorem 2 for fault sensitivity analysis in the presence of uncertainty. For checking the detectability condition presented in Theorem 2, we simply calculate the infimum of $\|\|x_{sub,i,j}(t_d) - \hat{x}_{sub,i,j}(t_d)\| - \|\tilde{x}_{sub,i,j}(t_d) - x_{sub,i}(t_d)\|\|$ for each residual and we call it the detectability constant, $\bar{\delta}$. If the detectability constant is more than value of its corresponding threshold, then the residual breaches its threshold. To this end, we consider a case where a small abrupt fault in $u_2 = T_0$ takes place at time $t_f = 7.5$ min. The simulated faults are as follows:

$$u_{f_2} = \begin{cases} 0, & 0 \leq t < t_f \\ 0.1, & t \geq t_f \end{cases} \tag{65}$$

The detectability constant and thresholds corresponding to each residual are shown in Table III. Since the detectability constants are less than threshold values for all of the residuals, therefore we expect that none of the residual breaches its threshold and the fault can not be detected. This is corroborated by the simulations.

We next consider a case where abrupt faults in $u_1 = C_{\mathrm{A0}}$ and $y_1 = C_{\mathrm{A}}$ (one actuator fault and one sensor fault) take place at time $t_f = 7.5$ min. The simulated faults are as follows:

$$\begin{aligned} u_{f_1} &= \begin{cases} 0, & 0 \leq t < t_f \\ 0.05, & t \geq t_f \end{cases} \\ y_{f_1} &= \begin{cases} 0, & 0 \leq t < t_f \\ 0.1, & t \geq t_f \end{cases} \end{aligned} \tag{66}$$

The evolution of residual profile is shown in Fig. 2. In this case the fault signature is breaching of all the residuals except r_{19} . Using the threshold designed in [6], some of the residuals breach their thresholds. In essence, the fault is successfully detected but is not isolated since the residual breaching profiles do not match any of the expected breaching patterns presented in [6]. In particular, while we expect only r_{19} be insensitive to the fault in u_1 and y_1, the residuals r_4, r_6, r_7, r_8, r_9, r_{10} and r_{11} are alway below the thresholds suggested in [6]. However, using the proposed threshold selection, only r_{19} does not breach its threshold, resulting in successful fault isolation in u_1 and y_1.

Prepared using rncauth.cls
DOI: 10.1002/rnc

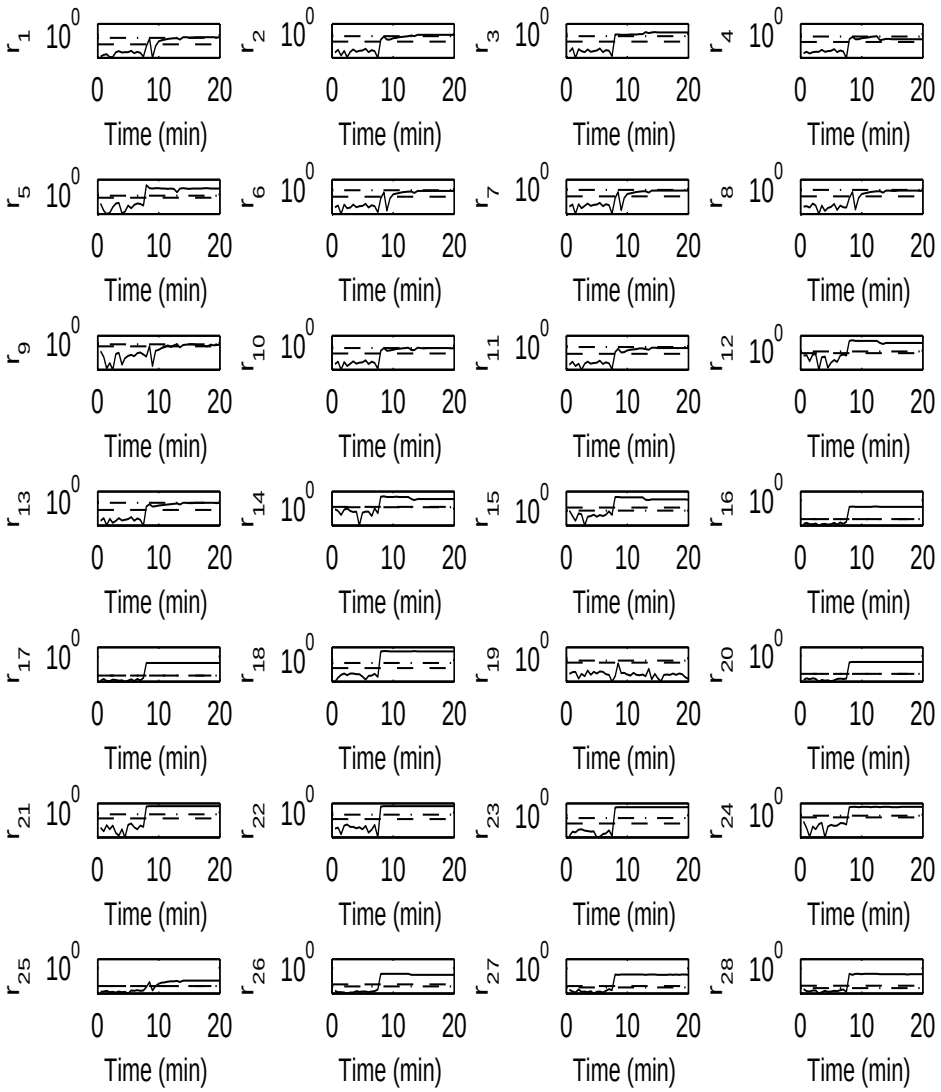

Figure 2. Evolution of the residuals (solid lines), thresholds (dashed lines) and thresholds designed in [6] (dashed-dotted lines). Using the thresholds proposed in [6], the residuals do not follow any of expected breaching patterns which results only in fault detection. By utilizing the thresholds designed in this work, all of the residuals breach their thresholds except for r_{19}. This corresponds to fault signature of fault only in u_1 and y_1 and as a result, faults in u_1 and y_1 are isolated.

Prepared using rncauth.cls
DOI: 10.1002/rnc

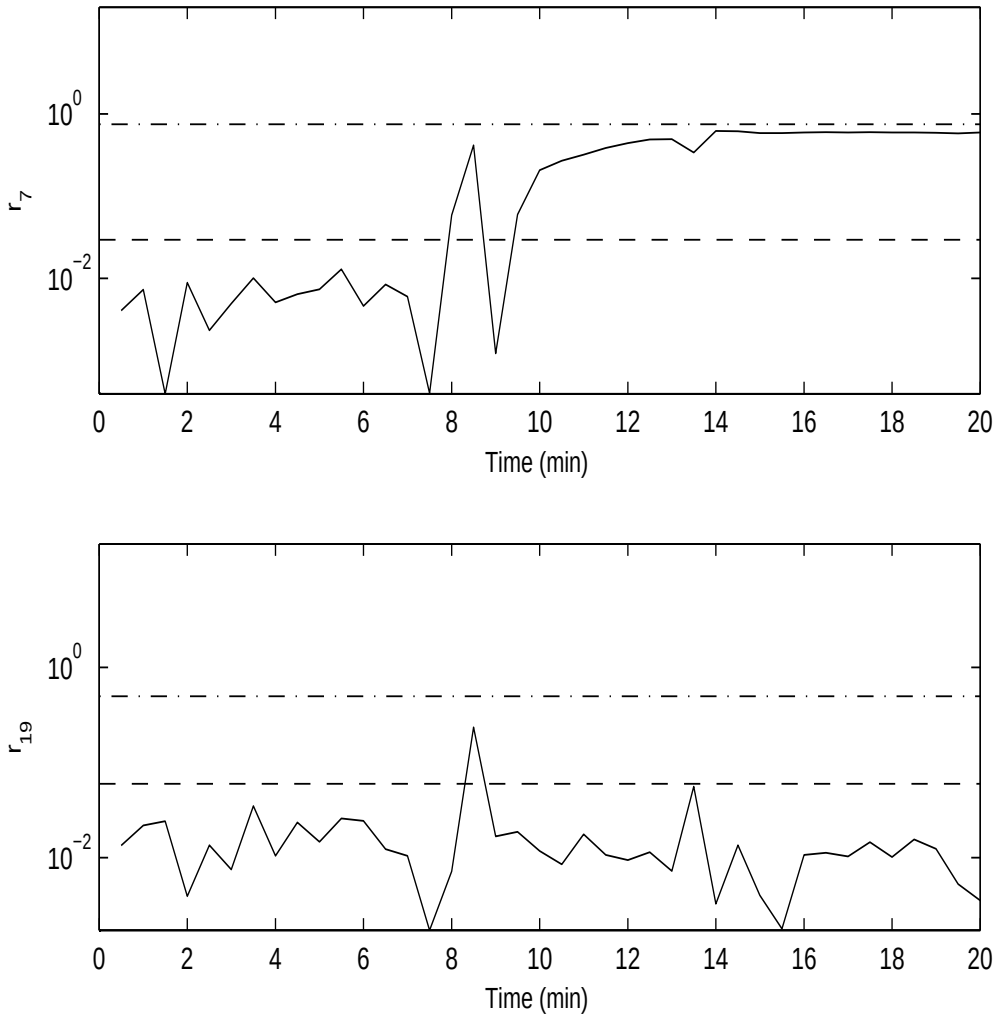

Figure 3. Evolution of the residuals for r_7 and r_{19} (solid lines), thresholds (dashed lines) and thresholds designed in [6] (dashed-dotted lines). Using the thresholds proposed in [6], both of the residual r_7 and r_{19} do not breach their thresholds which results only in fault detection. By utilizing the thresholds designed in this work, only r_{19} does not breach its threshold, matching a unique fault signature (see Table II), and as a result, the fault scenario is isolated.

As an example, the magnified version of evolution of residual profiles for r_7 and r_{19} are shown in Fig. 3.

Remark 10. Note that while residuals are defined using same methodology as proposed in [6], definition of thresholds is the key difference between the proposed scheme in this work and [6].

Prepared using rncauth.cls
DOI: 10.1002/rnc

In [6], thresholds are selected by using normal operating data for residuals plus some additional positive value to avoid false alarms due to plant model mismatch and uncertainty. This results in conservatively large values for thresholds and increased number of missed faults. However, by selecting thresholds as suggested by Eq. 28, the number of missed faults is reduced by explicitly accounting for the presence of uncertainty in the design. This is achieved by selecting the smallest possible values for thresholds while still guaranteeing that no false alarm before fault occurrence are triggered (see Fig. 2 for an illustration). Using thresholds values suggested in [6], the FDI scheme is not able to isolate the fault since the thresholds are selected conservatively large to avoid any false alarm, resulting in missing the location of the fault. In contrast, using the threshold values suggested in Table II, the fault is successfully isolated.

We next consider a case where incipient faults in $u_1 = C_{A0}$ and $y_5 = T_{\mathrm{R}}$ (one actuator fault and one sensor fault) take place at time $t_f = 7.5$ min. The simulated faults are as follows:

$$u_{f_2} = \begin{cases} 0, & 0 \leq t < t_f \\ (5 + 0.1\sin t)(1 - e^{t_f - t}), & t \geq t_f \end{cases}$$
$$y_{f_2} = \begin{cases} 0, & 0 \leq t < t_f \\ (0.2 + 0.2\sin t)(1 - e^{t_f - t}), & t \geq t_f \end{cases} \tag{67}$$

The evolution of residual profiles is shown in Fig. 4. The fault signature in this case is breaching of all of the residuals except r_{26}. Since all of the residuals breach their thresholds except r_{26}, which is designed to be insensitive to u_{f2} and y_{f2} (see Table II), faults in u_2 and y_2 are isolated.

6. CONCLUSIONS

In this work, we considered the problem of actuator and sensor fault detection and isolation of nonlinear systems subject to uncertainty. An FDI framework was proposed and fault detectability and isolability conditions were rigorously derived. Finally, the efficacy of the fault isolation framework subject to uncertainty and measurement noise was illustrated using a chemical reactor example. The future work could involve extending the proposed scheme to stochastic systems.

Prepared using rncauth.cls
DOI: 10.1002/rnc

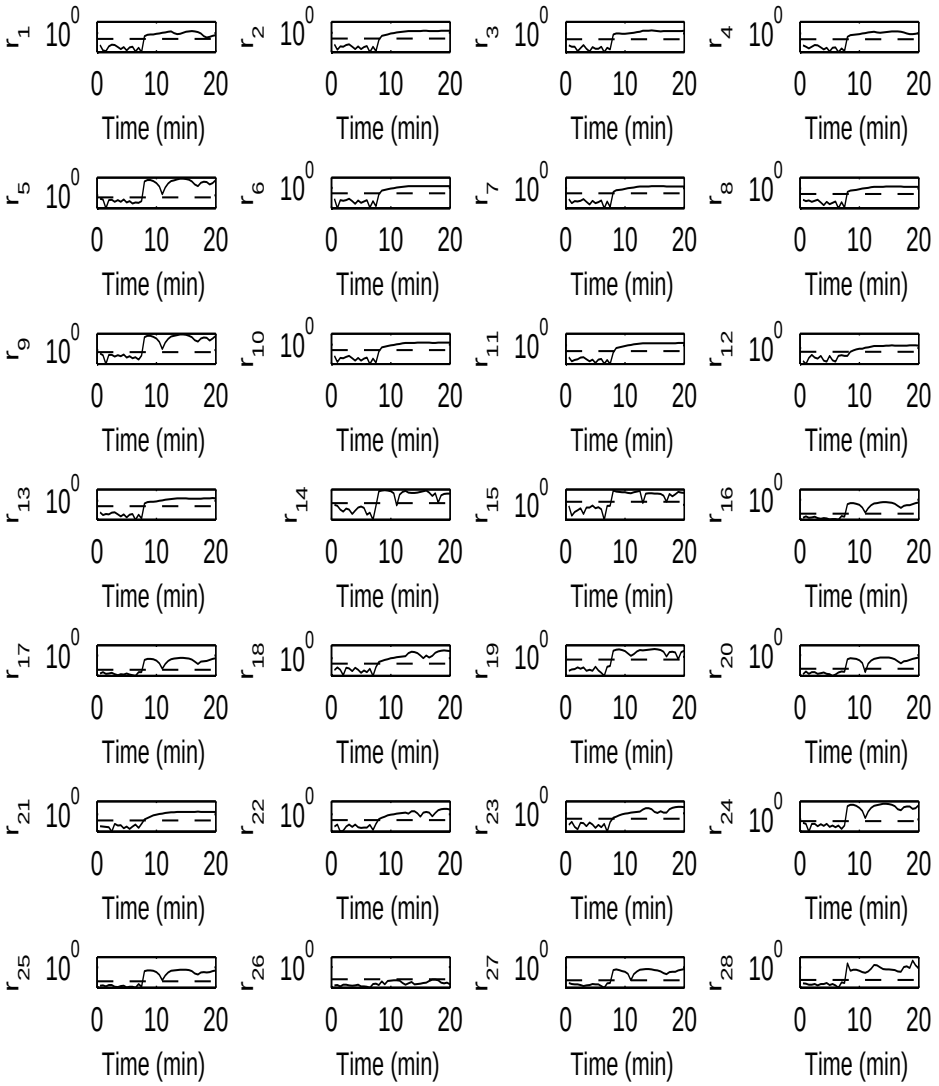

Figure 4. Evolution of the residuals (solid lines), thresholds (dashed lines). All the residuals breach their thresholds except for r_{26} matching the unique fault signature for a fault in u_2 and y_2 leading to fault isolation.

ACKNOWLEDGMENTS

Financial support from the McMaster Advanced Control Consortium is gratefully acknowledged.

REFERENCES

Prepared using rncauth.cls
DOI: 10.1002/rnc

1. P Kaboré, S Othman, TF McKenna, and H Hammouri. Observer-based fault diagnosis for a class of non-linear systems application to a free radical copolymerization reaction. *International Journal of Control*, 73(9):787–803, 2000.
2. Claudio De Persis and Alberto Isidori. A geometric approach to nonlinear fault detection and isolation. *Automatic Control, IEEE Transactions on*, 46(6):853–865, 2001.
3. R Kabore and Hong Wang. Design of fault diagnosis filters and fault-tolerant control for a class of nonlinear systems. *IEEE Transactions on Automatic Control*, 46(11):1805–1810, 2001.
4. Prashant Mhaskar, Charles McFall, Adiwinata Gani, Panagiotis D Christofides, and James F Davis. Isolation and handling of actuator faults in nonlinear systems. *Automatica*, 44(1):53–62, 2008.
5. M. Mattei, G. Paviglianiti, and V. Scordamaglia. Nonlinear observers with H_∞ performance for sensor fault detection and isolation: a linear matrix inequality design procedure. *Contr. Eng. Prac.*, 13:1271–1281, 2005.
6. Miao Du, James Scott, and Prashant Mhaskar. Actuator and sensor fault isolation of nonlinear process systems. *Chemical Engineering Science*, 104:294–303, 2013.
7. Miao Du and Prashant Mhaskar. Isolation and handling of sensor faults in nonlinear systems. *Automatica*, 50(4):1066–1074, 2014.
8. Di Peng, Nael H El-Farra, Zhiqiang Geng, and Qunxiong Zhu. Distributed data-based fault identification and accommodation in networked process systems. *Chemical Engineering Science*, 136:88–105, 2015.
9. Hadi Shahnazari and Prashant Mhaskar. Fault detection and isolation analysis and design for solution copolymerization of MMA and VAc process. *AIChE Journal*, 62(4):1054–1064, 2016.
10. Miao Du and Prashant Mhaskar. Active fault isolation of nonlinear process systems. *AIChE Journal*, 59(7):2435–2453, 2013.
11. Thierry Floquet, Jean-Pierre Barbot, Wilfrid Perruquetti, and Mohamed Djemai. On the robust fault detection via a sliding mode disturbance observer. *International Journal of control*, 77(7):622–629, 2004.
12. Xing-Gang Yan and Christopher Edwards. Nonlinear robust fault reconstruction and estimation using a sliding mode observer. *Automatica*, 43(9):1605–1614, 2007.
13. Antonios Armaou and Michael A Demetriou. Robust detection and accommodation of incipient component and actuator faults in nonlinear distributed processes. *AIChE Journal*, 54(10):2651–2662, 2008.
14. Xiaodong Zhang, Marios M Polycarpou, and Thomas Parisini. Fault diagnosis of a class of nonlinear uncertain systems with lipschitz nonlinearities using adaptive estimation. *Automatica*, 46(2):290–299, 2010.
15. Xiaodong Zhang. Sensor bias fault detection and isolation in a class of nonlinear uncertain systems using adaptive estimation. *Automatic Control, IEEE Transactions on*, 56(5):1220–1226, 2011.
16. Randy A Freeman and Petar V Kokotovic. *Robust nonlinear control design: state-space and Lyapunov techniques*. Springer Science & Business Media, 2008.
17. Jeffrey H Ahrens and Hassan K Khalil. High-gain observers in the presence of measurement noise: A switched-gain approach. *Automatica*, 45(4):936–943, 2009.

Prepared using rncauth.cls
DOI: 10.1002/rnc

18. Rolf Findeisen, Lars Imsland, Frank Allgöwer, and Bjarne A Foss. Output feedback stabilization of constrained systems with nonlinear predictive control. *International Journal of robust and nonlinear control*, 13(3-4):211–227, 2003.
19. Ahmad N Atassi and Hassan K Khalil. A separation principle for the stabilization of a class of nonlinear systems. *IEEE Transactions on Automatic Control*, 44(9):1672–1687, 1999.
20. Paul M Frank. Fault diagnosis in dynamic systems using analytical and knowledge-based redundancy: A survey and some new results. *Automatica*, 26(3):459–474, 1990.
21. Marios M Polycarpou and Alexander B Trunov. Learning approach to nonlinear fault diagnosis: detectability analysis. *Automatic Control, IEEE Transactions on*, 45(4):806–812, 2000
22. Jie Chen and Ron J Patton. *Robust model-based fault diagnosis for dynamic systems*, volume 3. Springer Science & Business Media, 2012.
23. Rolf Isermann. *Fault-diagnosis systems: an introduction from fault detection to fault tolerance*. Springer Science & Business Media, 2006.
24. Mogens Blanke and Jochen Schröder. *Diagnosis and fault-tolerant control*, volume 2. Springer, 2006.
25. Steven Ding. *Model-based fault diagnosis techniques: design schemes, algorithms, and tools*. Springer Science & Business Media, 2008

Prepared using rncauth.cls
DOI: 10.1002/rnc